*Diversity and Distributions*

WILEY

Diversity and Distributions

**RESEARCH ARTICLE** OPEN ACCESS

# Direct Integration of Population Genetics and Dynamic Species Distribution Modelling Improves Predictions of Post-Glacial History of *Piper nigrum*

Sandeep Sen[1,2,3] | Michael Peter Nobis[4] | Rani M.S. Saggere[2] | Srirama Ramanujam[2] | Thomson Davis[5] | Dirk Nikolaus Karger[4] | G. Ravikanth[2] | Yoshiaki Tsuda[1]

[1]Sugadaira Research Station, Mountain Science Center, University of Tsukuba, Nagano, Japan | [2]Ashoka Trust for Research in Ecology and the Environment (ATREE), Bengaluru, India | [3]Department of Ecosystem and Landscape Dynamics, Institute for Biodiversity and Ecosystem Dynamics, University of Amsterdam, Amsterdam, the Netherlands | [4]Swiss Federal Research Institute WSL, Birmensdorf, Switzerland | [5]Jawaharlal Nehru Tropical Botanical Garden and Research Institute (JNTBGRI), Trivandrum, India

**Correspondence:** Sandeep Sen (s.sen@uva.nl) | Michael Peter Nobis (michael.nobis@wsl.ch) | Yoshiaki Tsuda (tsuda.yoshiaki.ge@u.tsukuba.ac.jp)

**Received:** 15 January 2025 | **Revised:** 31 May 2025 | **Accepted:** 1 August 2025

**Editor:** Laura D. Bertola

**Funding:** This work was supported by JSPS Postdoctoral Fellowships for Research in Japan (Fellowship ID P20403), JSPS Kakenhi Grant-in-Aid for JSPS Fellows (22F20403), JSPS Kakenhi Grant in Aid for Scientific Research B (25K02056), JSPS Core to Core program: Asia-Africa Science Platforms B (JPJSCCB20220007), Grants from Yamazaki Spice Promotion Foundation in 2018, International Association for Plant Taxonomy (IAPT) and Department of Science and Technology (DST), India (YSS/2015/000234.Dated02/08/2018).

**Keywords:** black pepper | climate change | dynamic species distribution | hindcasting | phylogeography | Western Ghats

## ABSTRACT

**Aim:** Climate change has a strong impact on species ranges and the genetic structure of populations, yet conclusions are often subject to large uncertainties when both are analysed independently. Here, we develop a novel framework to directly integrate population genetics and dynamic species distribution modelling to reduce such uncertainties when reconstructing the post-glacial history of black pepper.

**Location:** Western Ghats, India.

**Methods:** Genetic data of 243 individuals from 14 populations of wild *Piper nigrum* were derived from six chloroplast and five nuclear DNA simple sequence repeats (SSRs). Dynamic species distribution models (DSDMs) were applied since the Last Glacial Maximum (LGM, 21,000 years BP) based on paleo-climatic suitability at a high resolution (1 km, 100 years) and evaluated for a wide range of estimated migration rates and climate niches of the species. Population genetics and DSDMs were finally combined in a genetically informed DSDM, in which the estimated model parameters were optimised by maximising the correlation between the genetic diversity of the populations and their simulated colonisation history since the LGM.

**Results:** We observed higher gene diversity, haplotype richness, and allelic richness at lower latitudes, and two major phylogeographic groups belonging to the southern and central Western Ghats. Demographic inference from chloroplast SSRs estimated the split of these groups around the LGM. DSDMs showed a high uncertainty in parameter estimates, which were clearly reduced for the genetically informed DSDM. With this model, the correlation between genetic diversity and colonisation time was

---

Sandeep Sen and Michael Peter Nobis contributed equally to this work.

G. Ravikanth and Yoshiaki Tsuda are co last authors.

stronger than the correlation with latitude, and the simulation showed a northward expansion from low-latitude refugia and a recent fragmentation of the species range.

**Main Conclusions:** Our integrative approach reduces uncertainty in DSDMs and facilitates the interpretation of the population genetic structure. This added value is not given when population genetics and species distribution modelling are applied independently and merely compared.

## 1 | Introduction

Quaternary climatic oscillation has reshaped species ranges and changed their genetic structure by altering, disconnecting, and reconnecting populations through time (Magri et al. 2006; Maiorano et al. 2013; Yannic et al. 2014; Flantua et al. 2019; Kirschner et al. 2022). Although many species are showing migration lags (Svenning and Skov 2004) and might not be able to track the rapid pace of current climate change (Corlett and Westcott 2013; Wang et al. 2023), for most species, a high uncertainty exists about how fast they can migrate or adapt to shifts in environmental conditions (Bellard et al. 2012; Meek et al. 2023; Rubenstein et al. 2023). To overcome such uncertainties, integrating population genetics and species distribution modelling can help to better understand the climatic impact on the past distributions of species and their current genetic diversity (McGaughran 2015; Tsuda et al. 2015). However, most studies compare the independent results from both fields (Smith et al. 2022; Kirschner et al. 2023), while only a limited number of studies have benefitted from the direct integration of population genetics and species distribution modelling (e.g., Espíndola et al. 2012; Brown et al. 2016; Yannic et al. 2020). The methodology of such integrative studies remains an active area of research (Gotelli and Stanton-Geddes 2015; Franklin 2023; Hernández et al. 2024), especially to inform how past climatic oscillation has influenced both species distributions and population genetic structuring, which has great potential to improve biodiversity conservation.

Inferences based on population genetics and species distribution modelling have both strengths and weaknesses in hindcasting past species distributions (Quinzin et al. 2017; Yannic et al. 2020). Regarding Quaternary climate change, population genetics has been shown to reveal the demographic history of populations (e.g., Boria and Blois 2023), the extent and timing of hybridisation (e.g., Tsuda et al. 2016, 2017), and lineages indicating a common history (e.g., Luna et al. 2023). At the same time, population genetic inferences are obscured by identifiability issues. For example, long-distance colonisation from a single refuge versus expansion from multiple refugia can lead to similar genetic structures, and recent bottlenecks or human activities may blur preexisting structures (Petit et al. 1997; Castilla et al. 2024).

A comparison with independently applied species distribution models (SDMs) can partly overcome such limitations (Tsuda et al. 2015; Leugger et al. 2022; Chiocchio et al. 2021). However, only a few studies have confirmed a positive correlation between SDM predictions and genetic diversity (Lee-Yaw et al. 2022). Static or correlative SDMs, also known as environmental niche models or habitat suitability models (Guisan et al. 2017), assume that the distribution of a species is in equilibrium with its environment. These models do not directly consider underlying processes like dispersal or population dynamics, nor do they explicitly model the dynamics of species ranges. Since these processes and dynamics often result in a disequilibrium between the species distribution and habitat suitability, which violates the model assumption of static SDMs and leads to biased predictions, it has been advocated to increasingly use dynamic, process-explicit models instead (Sandel et al. 2025). Different implementations of dynamic species distribution models (hereafter referred to as DSDMs) exist with a wide range of model complexity—from simple cellular automata and direct simulations of migration as a high-level dynamic to individual-based approaches considering basic processes like demography or dispersal (e.g., Engler and Guisan 2009; Nobis and Normand 2014; Bocedi et al. 2014, 2021; Shipley et al. 2022; Dobson et al. 2023). Most DSDMs do however also have disadvantages, because they are computationally expensive, the parameter estimates are not available for a given species, or these estimates come with a high uncertainty, which can hardly be evaluated in parameter space for more complex models. In addition, reliable model testing requires independent data, such as macro-fossils, pollen records, or population genetic data, and as with static SDMs such validations of DSDMs are often lacking and can affect conclusions for phylogeography and biodiversity conservation (Uribe-Rivera et al. 2023). The combined analysis of climate change impacts on both intra-specific genetic diversity and the dynamics of species distributions, therefore, has great potential in refining our understanding of distribution dynamics, demography and population structuring (Yannic et al. 2020; Leugger et al. 2022). With the recent development of paleoclimate data since the Last Glacial Maximum (LGM, 21,000 years before present (BP)) at a high spatio-temporal resolution (Karger et al. 2023), simulations of past species distributions can now be carried out more easily.

Here, we jointly examined the current genetic structure and the distribution dynamics of wild populations of the important spice crop black pepper (*Piper nigrum* L., Piperaceae) over the past 21,000 years. *Piper nigrum* is an endemic woody climber that has a tight association with the tropical evergreen forests of the Western Ghats, India. So far, no phylogeographic studies from this region have jointly used population genetics and DSDMs to infer the past demography and distributions of a species, although the global biodiversity hotspot in the Western Ghats and the regions nearby are known to have undergone dramatic changes during the Quaternary period (Prasad et al. 2009; Morley 2000). During the LGM, the sea level retracted by 120 m from the present level, exposing the continental shelf as vast open land surface on the southern coast with the presence of evergreen vegetation, including Piperaceae (Prabhu et al. 2004; Farooqui et al. 2014). It has been suggested that both the relatively humid mountain valleys and coastal areas on the western side of the Western Ghats could have served as refugia for wet-zone species during the not only colder but also drier LGM (Prasad et al. 2009; Farooqui et al. 2014; Bose et al. 2016). Phylogeographic analyses have documented, however, multiple yet contrasting response patterns to Quaternary climate change in the Western Ghats (see Robin et al. 2010; Bose et al. 2016; Nair et al. 2019; Chaitanya et al. 2025), and it is yet to be understood how much of these variations stems from differences in species' ecology or history, or from the different methods used.

The overall goal of our study, therefore, was to investigate the influence of climate change since the LGM on the distribution, genetic diversity, and phylogeographic patterns of *P. nigrum*, and to directly integrate the genetic diversity in the dynamic modelling of its past distribution. Specifically, our study had three major goals: (1) Infer the likely position of glacial refugia. We test the hypothesis that populations on the southern Western Ghats exhibit higher intraspecific genetic diversity under suitable climate since the LGM, supporting a long-term refugium in this region. (2) Identify the most likely migration routes since the LGM. Here we hypothesise that DSDMs and genetic data will indicate that the Western Ghats' coastal lowlands acted as an important migration route for *P. nigrum*. (3) Finally, develop a genetically informed DSDM by directly integrating population genetic diversity in the DSDM approach. For this integration, we assume a reduced uncertainty in the estimated model parameters and thus a more robust reconstruction of past distribution dynamics and more reliable conclusions on the impacts of past climate change.

## 2 | Methods

For this study, we first investigated the population genetic structure and phylogenetic groups of *P. nigrum* from the maternally inherited chloroplast and bi-parentally inherited nuclear simple sequence repeats (SSR) and estimated the demographic history using approximate Bayesian computation. We then developed different scenarios of the past distribution dynamics with different estimates of the climatic niche and the migration ability of the species using paleoclimate and a simple DSDM. In a final step, we directly integrated population genetics and the DSDM simulations by optimising the relationship between genetic diversity and the simulated colonisation history of the populations studied. Figure 1 shows an overview of this genetically informed DSDM approach.

### 2.1 | Study Area and Study Species

The Western Ghats escarpment is one of the world's eight most important hotspots of terrestrial biodiversity (Myers et al. 2000), and a global priority area for ecosystem restoration (Strassburg et al. 2020). Running along the western coast of Peninsular India (~1600 km in latitudinal extent), it is also densely populated by humans (> 300 persons/km$^2$, Cincotta et al. 2000; also see Das et al. 2006). Mountain peaks of the Western Ghats rise from north to south, providing strong environmental gradients, with the highest peak in the southern Western Ghats (Anamudi, 2695 m a.s.l.). The Western Ghats is separated by a geologically old (pre-Cambrian) 40-km-wide geographical gap known as the Palakkad gap (or Palghat gap) (Figures 2 and 3a). As one of the world's greatest escarpments (Rao and Kumar 2022), the western slopes receive high rainfall, providing enough habitat heterogeneity for lineages to radiate rapidly (Vijayakumar et al. 2016; Sen et al. 2019; Gopal et al. 2023, and references therein) leading to an extraordinarily rich biodiversity.

The wild populations of *P. nigrum* are distributed between latitudes of 8° N and 15° N in the Western Ghats (Figures 2 and 3a) and, unlike cultivated varieties, are mostly dioecious

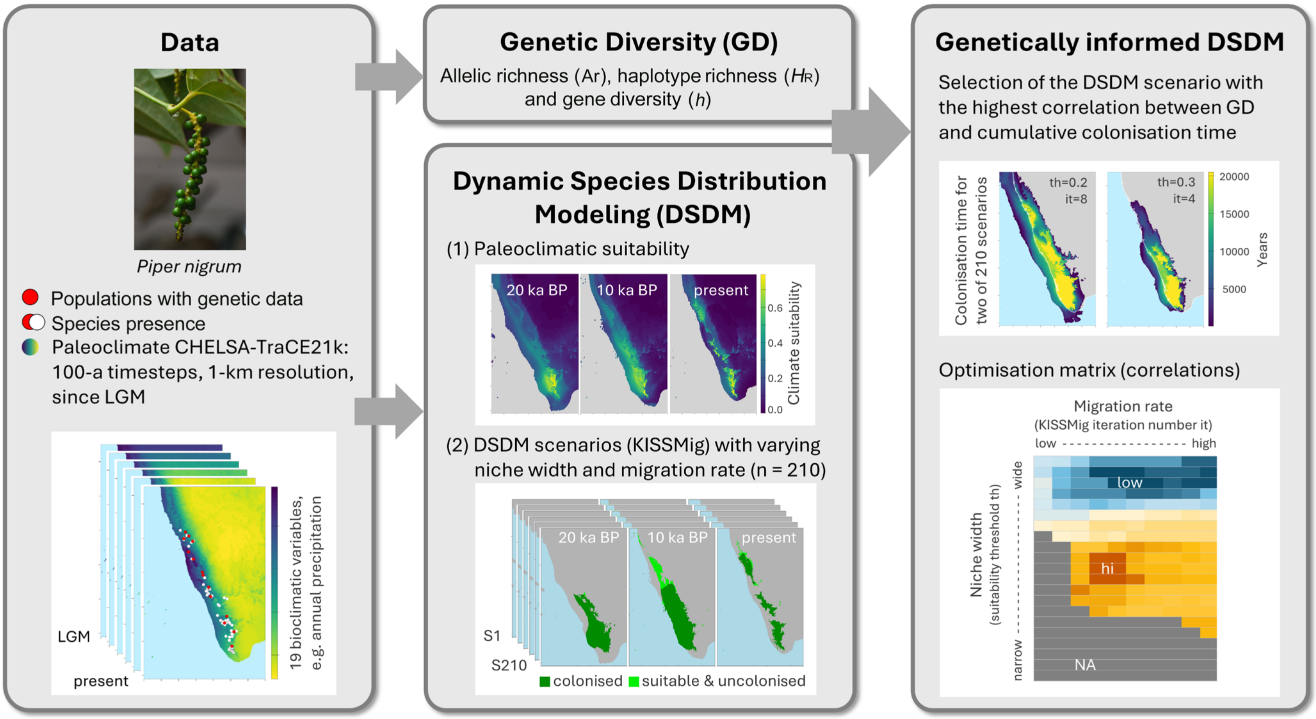

**FIGURE 1** | Overview of the study design, datasets and methods used for the genetically-informed dynamic species distribution model for black pepper (*Piper nigrum*).

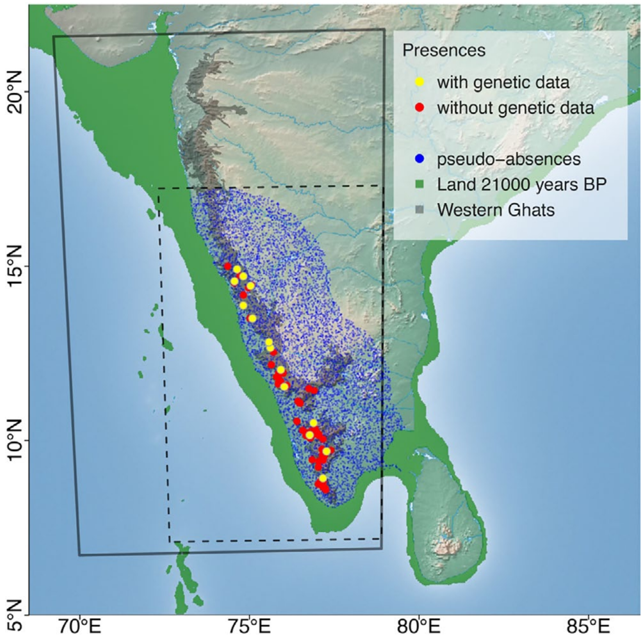

**FIGURE 2** | Map of Peninsular India with thinned presences ($N = 79$) of *Piper nigrum* and the pseudo-absences ($N = 7500$) used for ESM calibration. The green area was land 21,000 years before present (BP) and is now covered by the sea. The solid rectangle represents the extent of the dynamic species distribution modelling (KISSMig). The rectangle with the dashed line is the extent used for the calculation of the suitable versus colonised area and for the presentation of KISSMig results. All KISSMig simulations are based on data with Albers Equal Area projection as specified with further details in Appendix S3, Figure S3.1.

(Ravindran 2003; Sen and Rengaian 2022) and diverged from its sister species during the Miocene within the Western Ghats (Sen et al. 2019). The species is tetraploid ($2n = 4x = 52$), with the potential to propagate clonally (Ravindran 2003; Davis 2017). The peak flowering time coincides with the southwest monsoon season, and the flowers are mostly water pollinated, with instances of apomixis. The seeds are recalcitrant and dispersed by birds. Observations of cultivated individuals suggest that they attain reproductive maturity from 4 to 5 years after planting (Ravindran 2003), while the germination patterns in the species' natural habitats remain less explored.

## 2.2 | Field and Laboratory Methods

Leaf samples of 243 wild *P. nigrum* individuals were collected between 2012 and 2015 from 14 locations covering the entire natural range (~900 km; Table 1). All samples were wetted for taxonomic ambiguities before analysis. Leaf samples were dried, and genomic DNA was extracted using the DNeasy Plant Kit (Qiagen, Hilden, Germany). Ten universal chloroplast SSR (cpSSR) loci were screened (Weising and Gardner 1999), and two additional sets of cpSSRs were developed from the chloroplast genome sequence of *Piper cenocladum* C. DC. (genbank accession number: NC_008457.1). In addition, the nine published nuclear SSR (nSSR) loci developed for *P. nigrum* (Menezes et al. 2009) were genotyped (see Appendix S1, Table S1.1, for the details of sampling, primer sequences and the polymerase chain reaction (PCR) conditions and Appendix S2, Figure S2.1, for the leave-one-out test).

## 2.3 | Chloroplast Genetic Diversity and Structure

We used GenAlEx v6 (Peakall and Smouse 2006) to estimate the genetic diversity statistics gene diversity ($h$) and haplotype frequencies of cpSSRs. We employed GenoDive v3.0 (Meirmans 2020) to calculate haplotype richness ($H_R$, El-Mousadik and Petit 1996) using the rarefaction method based on a minimum sample size of 3 genes. The haplotype frequencies were plotted on the study area map using QGIS v3.6.0-Noosa. Pearson correlations of gene diversity and haplotype richness with latitude were calculated in R v4.4.1 (R Core Team 2024). To test for the phylogeographic signal, the population genetic differentiation statistics $G_{ST}$ (assuming an infinite allele model), $R_{ST}$ (considering the number of repeat differences and assuming a stepwise mutation model), and $N_{ST}$ (population subdivision based on phylogenetically ordered alleles) were measured and compared in the software Permut & cpSSR (Pons and Petit 1996).

Spatial analysis of molecular variance (SAMOVA; Dupanloup et al. 2002) was performed to infer population structure at the haploid cpSSR loci. A Neighbour-Net (NN; Bryant and Moulton 2004), implemented in SPLITSTREE4 (Huson and Bryant 2006), was employed to reconstruct phylogenetic relationships between cpSSR haplotypes using a pairwise uncorrected p-distance among samples. NN analysis was performed on two separate datasets: (a) including all the individuals of wild *P. nigrum*, the cultivars, and three wild species (*P. attenuatum* Buch.-Ham.ex Miq., *P. hymenophyllum* Miq. and *P. wightii* Miq.) (Appendix S2, Figure S2.2) and (b) with only the wild populations of *P. nigrum*. In addition, a neighbour-joining phylogenetic tree of the haplotypes was reconstructed based on the $(\delta\mu)^2$ distance (Goldstein et al. 1995) in the program POPULATIONS v1.2.31 (Langella 1999). The resulting tree was plotted on a map of the study area using the software GenGIS2 (Parks et al. 2013). Further, $F'_{ST}$ (Meirmans and Hedrick 2011), among the groups, and among populations within groups was evaluated by analysis of molecular variance (AMOVA) in GenoDive v3.0 (Meirmans 2020).

## 2.4 | Nuclear Genetic Diversity and Structure

Genetic diversity indices (gene diversity $h$ and allelic richness Ar) from nSSRs were calculated using GenoDive (Meirmans 2020), which can accept polyploid data. We applied the rarefaction method based on a minimum sample size of 28 genes. Population differentiation statistics, such as $F_{ST}$ and the standardised values of $F'_{ST}$ (Hedrick 2005), were calculated and implemented using GenoDive after correcting for unknown dosage of alleles. The latitudinal relationships of $h$ and Ar were assessed using Pearson correlations in R. A Mantel test was performed to estimate the isolation by distance (IBD) (Wright 1943; Rousset 1997), between geographic distance and pairwise population differentiation ($F_{ST}/(1\text{-}F_{ST})$) among populations, and its significance was determined using 999 permutations. The geographic distances were calculated using the R package *geosphere* (Hijmans 2019). METAPOP2 (López-Cortegano et al. 2019) was used to measure the relative contribution of each sampled population to the total allelic diversity ($A_T$) and its within sub-population and among sub-populations differentiations by treating a tetraploid

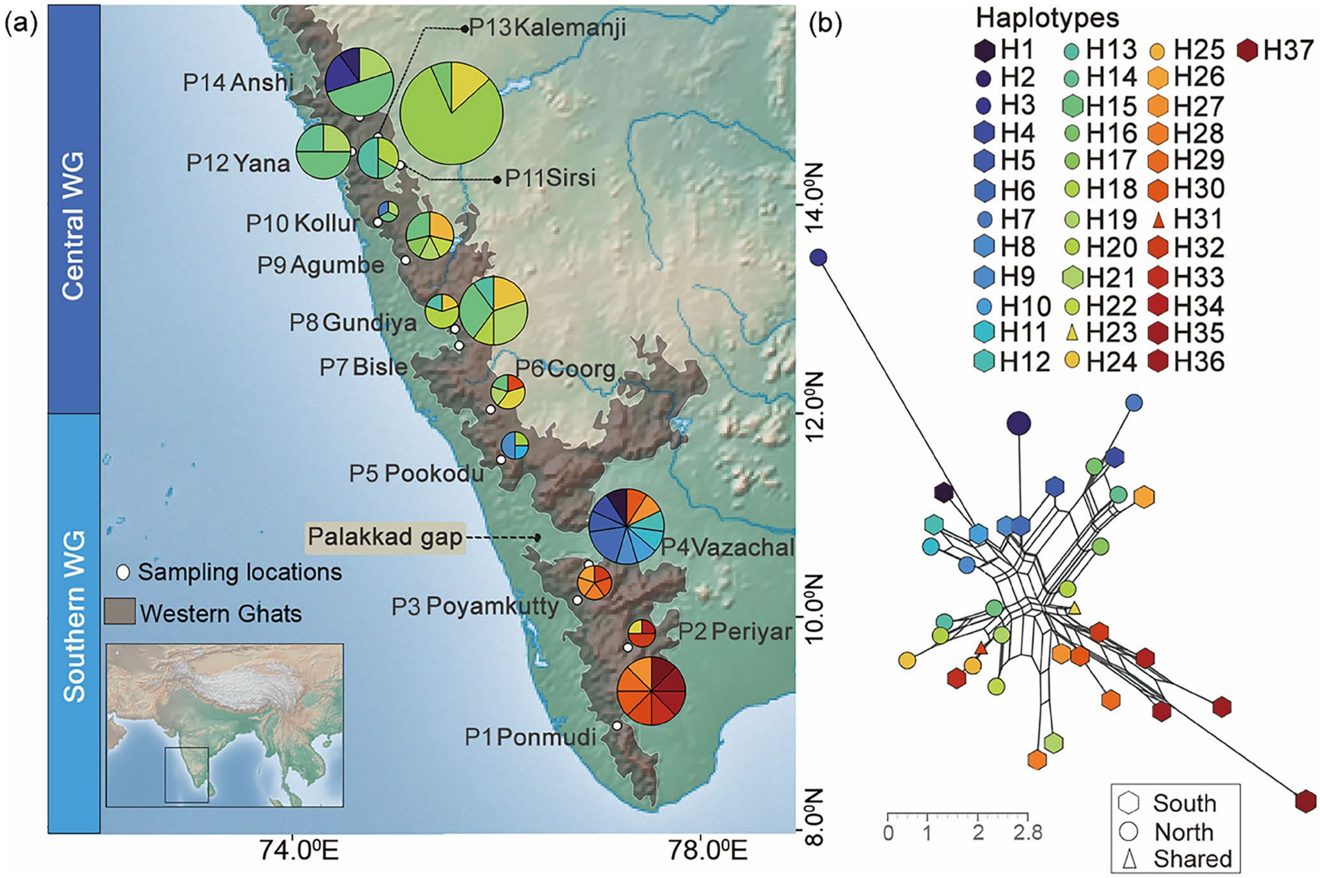

**FIGURE 3** | (a) Map of the distribution of sampling locations and the frequency of 37 chloroplast haplotypes across 14 populations of wild *P. nigrum* in the Western Ghats (area in dark grey). The size of each pie diagram corresponds to the sample size of a population. (b) Neighbour-net diagram showing the relationship between different haplotypes. Hexagons represent the haplotypes found in the southern Western Ghats, and circles indicate haplotypes from the central Western Ghats, that is, north of the Palakkad gap. Triangles indicate haplotypes shared between the central and southern Western Ghats. Haplotype 23 is shared between the Periyar (P2), Coorg (P6) and Sirsi (P11) populations, and H31 between the Ponmudi (P1) and Coorg (P6) populations (see also Appendix S4).

genotype as two diploid genotypes (see Tsuda et al. 2017 and Appendix S4). Here $A_S$ is the mean number of alleles occurring in each population, $D_A$ is the mean number of alleles in one population but absent in other populations, and $A_T$ is the sum of $A_S$ and $D_A$. To account for uneven sample sizes among populations, we applied rarefaction during the analysis.

The genetic structure of populations was estimated using the Bayesian clustering algorithm in STRUCTURE v2.3.4 (Pritchard et al. 2000; Falush et al. 2007; Hubisz et al. 2009) on the complete dataset of all individuals ($N = 243$) and setting ploidy = 4. The genetic relationships among the clustered populations were evaluated using a neighbour-joining phylogenetic tree of the clusters in STRUCTURE (see Appendix S2 for the details).

## 2.5 | Demographic History

Demographic analysis was performed based on the genetic clusters identified by SAMOVA using cpSSR loci only (see Section 3). To infer the demographic history of the wild populations of *P. nigrum*, six plausible scenarios were evaluated using approximate Bayesian computation (ABC) implemented in DIYABC v2.1 (Cornuet et al. 2008, 2014). In scenario 1, the southern group (Pop1) effective population size N1 was ancestral to the central group (Pop2) with an effective population size N2, and it derived from Pop1 at a historical time t1 ($N1 \geq N2$). In scenario 2, we considered an unknown ancestral population size (Na; $Na > N1$) from where Pop1 and Pop2 split at time t1. In scenario 3, we considered that Pop1 and Pop2 diverged from an ancestral population Nb (here $Nb < N1$). Scenario 4 assumes Pop2 as ancestral and Pop1 diverged from Pop2 ($N2 \geq N1$) at the historical time. Scenario 5 had Pop1 and Pop2 diverging at time t2 from an unknown population Nc ($Nc > N2$). In scenario 6, Pop1 and Pop2 diverged at time t2 from an unknown population Nd ($Nd < N2$) (see Appendix S2, Figures S2.3–S2.5 and Tables S2.1–S2.4 for the details). We observed high genetic differentiation ($F'_{ST}$) values among the haplotypes between Pop1 and Pop2 (see Section 3). Hence, our proposed models do not assume migration between genetic clusters. Since the number of polymorphic nuclear markers in this study was low, we refrained from a separate demographic analysis and restricted our discussion to the cpSSR dataset.

**TABLE 1** | Genetic summary statistics calculated for chloroplast and nuclear simple sequence repeats (cpSSRs and nSSRs) for the wild populations of *Piper nigrum*.

| | | | | Genetic diversity | | | |
|---|---|---|---|---|---|---|---|
| | | | | cpSSR | | nSSR | |
| **Population** | **Sample size** | **Latitude (°*N*)** | **Longitude (°*E*)** | ***h*** | $H_R$ | ***h*** | **Ar** |
| P1, Ponmudi | 18 (10) | 8.926 | 77.166 | 0.933 | 6.25 | 0.663 | 3.925 |
| P2, Periyar | 22 (4) | 9.696 | 77.273 | 0.833 | 2.667 | 0.701 | 3.656 |
| P3, Poyamkutty | 10 (5) | 10.160 | 76.776 | 0.982 | 9.308 | 0.742 | 4.755 |
| P4, Vazachal | 32 (11) | 10.509 | 76.889 | 1.000 | 5.000 | 0.726 | 3.832 |
| P5, Pookodu | 10 (4) | 11.542 | 76.027 | 0.833 | 2.667 | 0.762 | 4.039 |
| P6, Coorg | 14 (5) | 12.035 | 75.924 | 0.900 | 3.571 | 0.712 | 3.866 |
| P7, Bisle | 24 (10) | 12.663 | 75.615 | 0.844 | 4.167 | 0.735 | 4.642 |
| P8, Gundiya | 20 (5) | 12.825 | 75.575 | 0.700 | 2.273 | 0.682 | 4.048 |
| P9, Agumbe | 18 (7) | 13.502 | 75.090 | 0.905 | 4.455 | 0.652 | 3.881 |
| P10, Kollur | 7 (3) | 13.875 | 74.817 | 1.000 | 3.000 | 0.649 | 3.834 |
| P11, Sirsi | 22 (15) | 14.436 | 75.034 | 0.362 | 1.519 | 0.624 | 3.157 |
| P12, Yana | 9 (8) | 14.569 | 74.558 | 0.714 | 2.667 | 0.622 | 3.319 |
| P13, Kalemanji | 11 (6) | 14.712 | 74.819 | 0.733 | 2.571 | 0.555 | 2.525 |
| P14, Anshi | 26 (10) | 14.911 | 74.636 | 0.733 | 2.941 | 0.692 | 4.455 |
| Total | 243 (103) | | Mean | 0.819 | 3.789 | 0.679 | 3.852 |

*Note:* Values inside the parentheses in the sample size column represent the number of samples genotyped for cpSSRs. For chloroplasts, genetic diversity within the population was measured based on cpSSR haplotypes. Ar is allelic richness after correcting for unknown dosage, and *h* is the gene diversity and $H_R$ is the haplotype richness. Mean values were estimated from 103 and 243 samples for cpSSRs and nSSRs, respectively. The populations P1 to P14 are ordered by increasing latitude.

### 2.6 | Simulation of Post-Glacial Distribution Dynamics

A raster-based DSDM, KISSMig (Nobis and Normand 2014), was applied to simulate distribution dynamics of *P. nigrum* on top of binary paleoclimate suitability maps. KISSMig is a simple DSDM that starts from an initial species distribution and simulates extinction and colonisation events at the level of neighbouring raster cells on top of a time series of suitability maps. Paleoclimate data were derived from CHELSA-TraCE21k (Karger et al. 2021, 2023), which provides monthly climatologies and 19 bioclimatic variables for the last 21,000 years at a spatial resolution of 30 arcsec and in 100-year timesteps. CHELSA-TraCE21k bioclimatic variables were projected to Albers Equal Area (Appendix S3, Figure S3.1) by bilinear interpolation and with a spatial resolution of 1 km. An ensemble of small models (ESM; Breiner et al. 2015) was then built, with Maxent as the modelling technique, calibrated for 79 species presences covering the entire native range of *P. nigrum* along with 7500 pseudo-absences in their 250-km neighbourhood (Figure 2 and Figure S3.1). Presences were derived from an initial set of 97 coordinates (Table S3.1), after setting the minimum distance among the presences and between the presences and pseudo-absences to 2 km. Because paleoclimate data varied considerably over the last centuries (Figure S3.2), and species do not track climate change instantly, the ESM was calibrated for the average bioclimate between 1500 and 1990 (the last five CHELSA-TraCE21k layers) using five temperature- and precipitation-related predictors with low bivariate correlations ($|r| < 0.7$, Dormann et al. 2013; Figure S3.3): mean daily minimum air temperature of the coldest month (bio6), mean daily mean air temperature of the warmest quarter (bio10), annual precipitation (bio12), mean monthly precipitation of the driest quarter (bio17), and mean monthly precipitation of the warmest quarter (bio18). The calibrated ESM was used to predict a time series of 210 paleoclimate suitability maps since the LGM.

Past distribution dynamics were simulated by running KISSMig on top of these suitability maps after binarisation into climatically suitable and unsuitable raster cells. All cells that were climatically suitable in one of the first five suitability maps since LGM defined the initial distribution, and the stack of the remaining 205 layers was then used to simulate the distribution dynamics starting from this origin until today. Although the binarisation threshold can easily be optimised using the current presence–pseudo-absence data, it may not be the optimal threshold for simulations of the past due to the potential disequilibrium between the current species distribution and the environment. In addition, the migration ability of *P. nigrum* was unknown a priori. Various KISSMig simulations were therefore carried out with 21 different suitability thresholds (i.e., for a range of 0.2 and steps size 0.01 around the optimised threshold based on true skill statistic, TSS; values are specified in Results) and varying migration ability (i.e., KISSMig iteration numbers from 1 to 10, which corresponds to a maximum migration distance from 1 to 10 km per

100-year timestep). The simulated final species distribution for all 210 combinations of different suitability thresholds and migration abilities was evaluated using TSS and the current presence–pseudo-absence data.

### 2.7 | Integrating Population Genetics Into Simulations of Species Distribution Dynamics

In addition to the simulated distribution dynamics, the number of years each raster cell was colonised after the LGM (based on the KISSMig output 'number of occurrences'), hereafter called 'cumulative colonisation time', was recorded and mapped for each combination of suitability threshold and migration ability. Although we need to consider the effect of admixture and secondary contact, it can be assumed that genetic diversity, particularly allelic richness, is generally higher in the refugial areas where the populations have been present for a long time than in newly colonised areas (Comps et al. 2001; Petit et al. 2003; Hoban et al. 2010). Therefore, for all 210 simulations with varying suitability thresholds and migration rates, the relationships between the cumulative colonisation time and the genetic diversity estimates ($h$ and $H_R$ *for* cpSSRs and $h$ and Ar for nSSRs, respectively) were evaluated using Spearman correlations, and the maximum correlation was identified for each of the four genetic diversity estimates as well as their average correlation. All KISSMig-related simulations and visualisations were performed in R v4.4.1 (R Core Team 2024) using the package *kissmig* v1.0–5 (Nobis 2024) and the R packages listed in the Appendix S3.

## 3 | Results

### 3.1 | Genetic Diversity and Population Structure From cpSSRs

Out of the 12 screened cpSSRs, six (ccmp2, ccmp3, ccmp5, ccmp6, cptri, cptet) showed consistent PCR amplification. A total of 37 haplotypes were detected across all the loci among the wild populations (Figure 3; Appendix S4, Table S4.1). Significant phylogeographic structuring was detected with the cpSSR where $N_{ST}$ (population subdivision based on phylogenetically ordered alleles) and $R_{ST}$ (assuming a stepwise mutation model) values were significantly higher than $G_{ST}$ (assuming an infinite allele model; $N_{ST} = 0.349 > G_{ST} = 0.142$, $p < 0.05$; $R_{ST} = 0.313 > G_{ST} = 0.142$, $p < 0.05$). Furthermore, we observed a significant decreasing trend toward northern latitudes among haplotype richness ($H_R$) and gene diversity ($h$) ($p < 0.05$, Figure S4.1). We observed higher gene diversity and haplotype richness among the southern populations. $F_{ST}$ and $F'_{ST}$ values among populations were 0.304 ($p < 0.005$) and 0.436, respectively, showing a significant moderate genetic differentiation. A significant relationship between gene diversity and haplotype richness was observed for cpSSRs ($r = 0.63$, $p < 0.05$; Figure S4.2a).

SAMOVA recovered three genetic clusters displaying the highest $F_{CT}$ values, indicating the greatest differentiation among groups. The $F_{CT}$ values rose steadily from $K = 6$ onwards, reaching stationarity (Figure S4.3). At $K = 3$ ($F_{CT} = 0.253$), one cluster mostly belongs to the south of the Palakkad gap, a second to the north of the Palakkad gap, and a third widespread cluster found across the range (referred to as south, north and widespread cluster; Figure S4.4) respectively. At $K = 4$ onwards, single populations were forming groups (loss of between-population clustering), violating the assumption of SAMOVA. Hence, we interpret our results based on $K = 2$ ($F_{CT} = 0.342$), as it has clear biological explanations (as suggested by Meirmans 2015). $F'_{ST}$ values between haplotypes of the two groups identified by SAMOVA were 0.97, indicating high differentiation due to the almost nonsharing of haplotypes between the groups. These two clusters belong to southern (8° N–12° N) and the central Western Ghats (12° N–16° N) respectively. The phylogeny of haplotypes based on the $(\delta\mu)^2$ distance (Goldstein et al. 1995) identified similar genetic clustering, as identified by SAMOVA (Figure 4a and Figure S4.4).

### 3.2 | Genetic Diversity and Population Structure From nSSRs

Out of the nine microsatellites, five showed consistent amplification and polymorphisms and were selected for the genetic analysis (i.e., PN A5, PN D10, PN E3, PN G11 and PN F1). The population differentiation statistics $F_{ST}$ and $F'_{ST}$ were 0.098 and 0.325, respectively. Allelic richness (Ar) and gene diversity ($h$) from five nSSRs were lower in the northern latitudes (Figure S4.1), where gene diversity showed a significant negative correlation with latitude ($r = -0.58$, $p < 0.05$). Results of the Mantel test suggest a significant range-wide IBD among wild populations of *P. nigrum* ($r = 0.67$, $p < 0.01$). Ar and $h$ from nSSRs also showed a positive correlation among the study populations ($r = 0.82$, $p < 0.01$, Figure S4.2b). The results from AMOVA revealed that most of the genetic differentiation (72.1%) was found within populations. The population Bisle (P7) contributed most to the total allelic diversity ($A_T = 2.698$), followed by Anshi (P14; $A_T = 1.898$) while the northern population Kalemanji (P13) contributed the least ($A_T = -3.171$). Bisle also had the largest $A_S$ values (1.441) while the subpopulation Kalemanji showed the lowest $A_S$ (−1.977) (Figure S4.5).

In the STRUCTURE analysis, the probability of the data LnP(D) peaked at $K = 2$ based on Evanno et al. (2005). At $K = 2$, two distinct genetic clusters were observed: one major cluster in the southern Western Ghats and the other in the central Western Ghats. At $K = 3$, from the central Western Ghats northwards, populations formed a different genetic group, with some admixture among central populations. At $K = 4$, a new cluster emerged north and south of the Palakkad gap. From $K = 5$ to $K = 7$, these groupings become clearer, and the central Western Ghat populations emerged as a different genetic group (Figure 5). From $K = 8$ onwards, we observed complex multimodalities, and the assignment of individuals to clusters was inconsistent.

### 3.3 | Demographic History

In DIYABC, the highest posterior probability was for scenario 6 and the value (0.484, 95% CI: 0.473–0.495) which was much higher than for the second-best performing scenario 3 (0.350, 95% CI: 0.339–0.361), and its 95% CI did not overlap

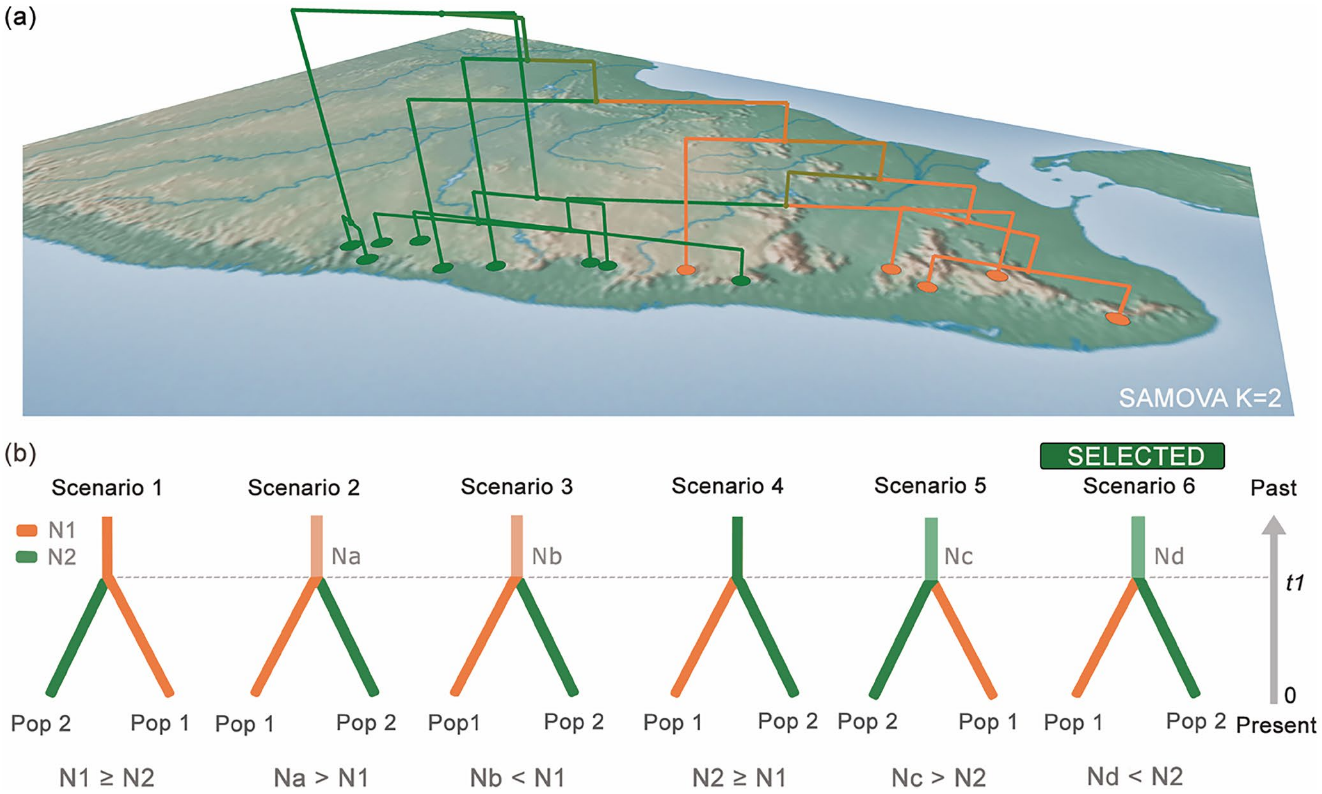

**FIGURE 4** | Population structure and demographic history from cpSSRs. (a) The neighbour joining phylogenetic tree of the haplotypes based on the $(\delta\mu)^2$ distance (Goldstein et al. 1995) superimposed on a map of the study area. Branches were coloured following the results of SAMOVA $K=2$. (b) six demographic scenarios tested in this study in DIYABC v2.1.0. The time scale here is measured in number of generations; the effective population size of Pop1 = N1, Pop2 = N2, Na–Nd represents an unknown ancestral population with varying effective population sizes.

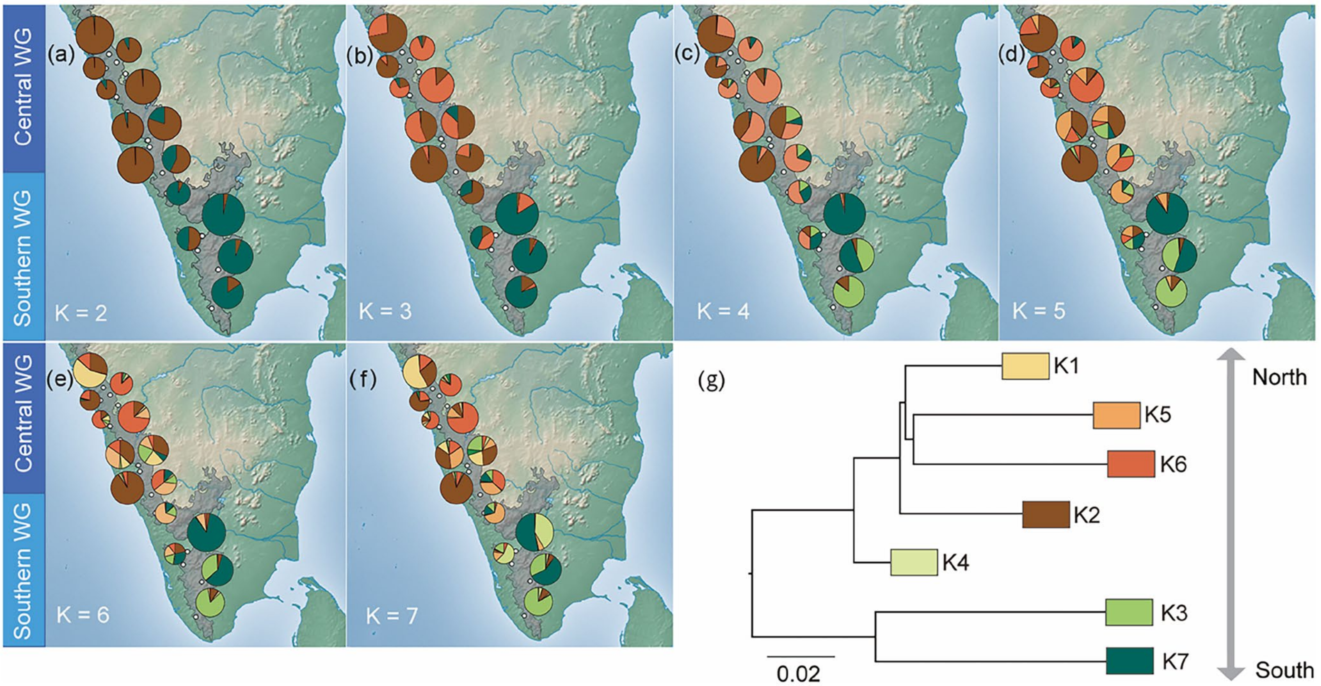

**FIGURE 5** | Genetic structure and a neighbour-joining tree of inferred clusters for 14 populations of wild *Piper nigrum* from the Western Ghats. (a–f) Pie diagrams of nuclear genetic clusters from $K=2$ to $K=7$ on a map of the Western Ghats. (g) neighbour-joining phylogenetic tree of seven inferred clusters from the STRUCTURE analysis.

with those of the other scenarios (Table S2.4). For scenario 6, the median values of effective population size of N1 (southern populations), N2 (central populations) and Nd (unknown ancestral populations) were 21,400 (95% CI: 11,100–29,500), 14,300 (95% CI: 7170–19,700), 3660 (95% CI: 205–9420) (Table S2.4). The median values of the mean mutation rate per generation of SSRs under the GSM and SNI models were estimated to be $5.95\times10^{-5}$ (95% CI: $2.36\times10^{-5}$–$9.80\times10^{-5}$), $2.03\times10^{-1}$ (95% CI: $1.09\times10^{-1}$–$2.95\times10^{-1}$), respectively. The PCA of DIYABC showed that the observed dataset (yellow) was in the centre of the posterior predictive distribution (Figure S2.3), suggesting that the observed data is generally close to the simulated data and thus scenario 6 fits the observed data well. Scenario 6 suggests a small ancestral population size for the central Western Ghats from which the populations of southern Western Ghats diverged around LGM (Figure 4b). The median value of the generation time indicating the split between the southern and central populations (t1) was 4790 generations ago (95% CI: 1580–9500). Assuming a generation time of 4 years for *P. nigrum*, the divergence time of these populations corresponded to 19,160 years BP, or 14,370 years BP and 23,950 years BP if we assumed generation times of 3 and 5 years, respectively (Ravindran 2003; personal observations SS).

### 3.4 | Simulation of Post-Glacial Distribution Dynamics (Without Genetics)

The calibrated ESM showed for the current species distribution three isolated patches of suitable area—one south and two north of the Palakkad gap. The model performed well, with an area under the curve (AUC) of 0.944, sensitivity of 0.937, and specificity of 0.833. The optimised TSS of the ESM ($\mathrm{TSS}_{\mathrm{ESM}}$) was 0.769, with a corresponding suitability threshold of 0.25. Since the optimised threshold value for the final DSDM was higher (see next chapter), KISSMig simulations with 21 threshold values between 0.20 and 0.40 and a step size of 0.01 were evaluated. For the final distribution of these simulations, the highest TSS value was 0.772, with a suitability threshold of 0.26 and an iteration number of three (Figure 6a). These TSS values generally varied only slightly but showed a sudden decline toward high suitability thresholds or low iteration numbers. Figure 6b indicates that, for such parameter combinations, not all populations were colonised during the simulation because the suitability threshold was too high, or the assumed migration ability of the species was too low.

### 3.5 | Integrating Population Genetics in the Simulation of Distribution Dynamics

The average Spearman correlation between the four genetic diversity estimates and the cumulative colonisation time varied among the different parameter combinations (Figure 6b). They showed a clear pattern, with the highest average correlations for suitability thresholds between 0.29 and 0.31 and the migration ability corresponding to iteration numbers of four or five. The highest correlation for a single genetic diversity measure was found for nuclear gene diversity ($r_s = 0.780$, $p < 0.001$; Appendix S4, Figure S4.6). For comparison, the Spearman correlation of nuclear gene diversity with latitude was only −0.631 ($p < 0.05$). We chose, therefore, the corresponding suitability threshold (th = 0.29) and iteration number (it = 4) as the optimised values for the genetically informed DSDM. This simulation also indicated a clear relationship ($R^2 = 0.55$) in a linear regression of nuclear gene diversity against log-scale cumulative colonisation time, with high values of both cumulative colonisation time and nuclear gene diversity in the southern Western Ghats (Figure 7a).

For the genetically informed DSDM, the change in colonised area since the LGM often lagged significantly behind the climatically suitable area—especially since sudden climatic changes and climate fluctuations since 15,000 years BP (Figures 7b–d). For comparison, the corresponding map of the cumulative colonisation time for the best-performing simulation without genetic information, that is, based on the optimised TSS (th = 0.26, it = 3), suggests—due to the lower threshold value—a persisting refugial area in the north, which is not present in the genetically informed DSDM, and therefore not supported by it (Appendix S4, Figure S4.7).

## 4 | Discussion

A joint inference of population genetics and our novel genetically informed DSDM located the LGM refugial area of *Piper nigrum* with high confidence. Besides, our study provides indications for possible migration routes of *Piper nigrum* within the Western Ghats hotspot in the past. These results jointly offer unique insights into how biodiversity in this area might have been (re)structured in response to past climatic oscillations. By inferring the past dynamics of *Piper nigrum*, a climbing species that colonises tropical evergreen forests, our results contribute to understanding how tropical forests might have responded to past climatic oscillations. Below we discuss the major findings and limitations of our results from the Western Ghats and the novel modelling approach, and their implications for biodiversity conservation.

### 4.1 | LGM Refugia and Migration Routes

The projected distribution of the genetically informed DSDM around LGM suggests that *P. nigrum* was more widely spread than today and that suitable climatic conditions prevailed through the LGM to the Holocene throughout the western coast of Peninsular India. The simulations revealed an overall reduction in suitable area until c. 15,000 BP and the absence of the species in the northern part of its extant distribution during that time. The climatically suitable area increased afterwards rapidly, due to a transition to more humid climate conditions (Tiwari et al. 2011). Because of the indicated bottleneck until c. 15,000 BP, suitable areas north of the extant distribution probably were not colonised rapidly, due to migration constraints.

In support of this simulation, the genetic structure of both the chloroplast and nuclear genome revealed two clusters in the southern and central Western Ghats. A similar pattern was previously observed in at least two other taxa, in the tree *Dysoxylum malabaricum* by Bodare et al. (2013) and in the flying lizard

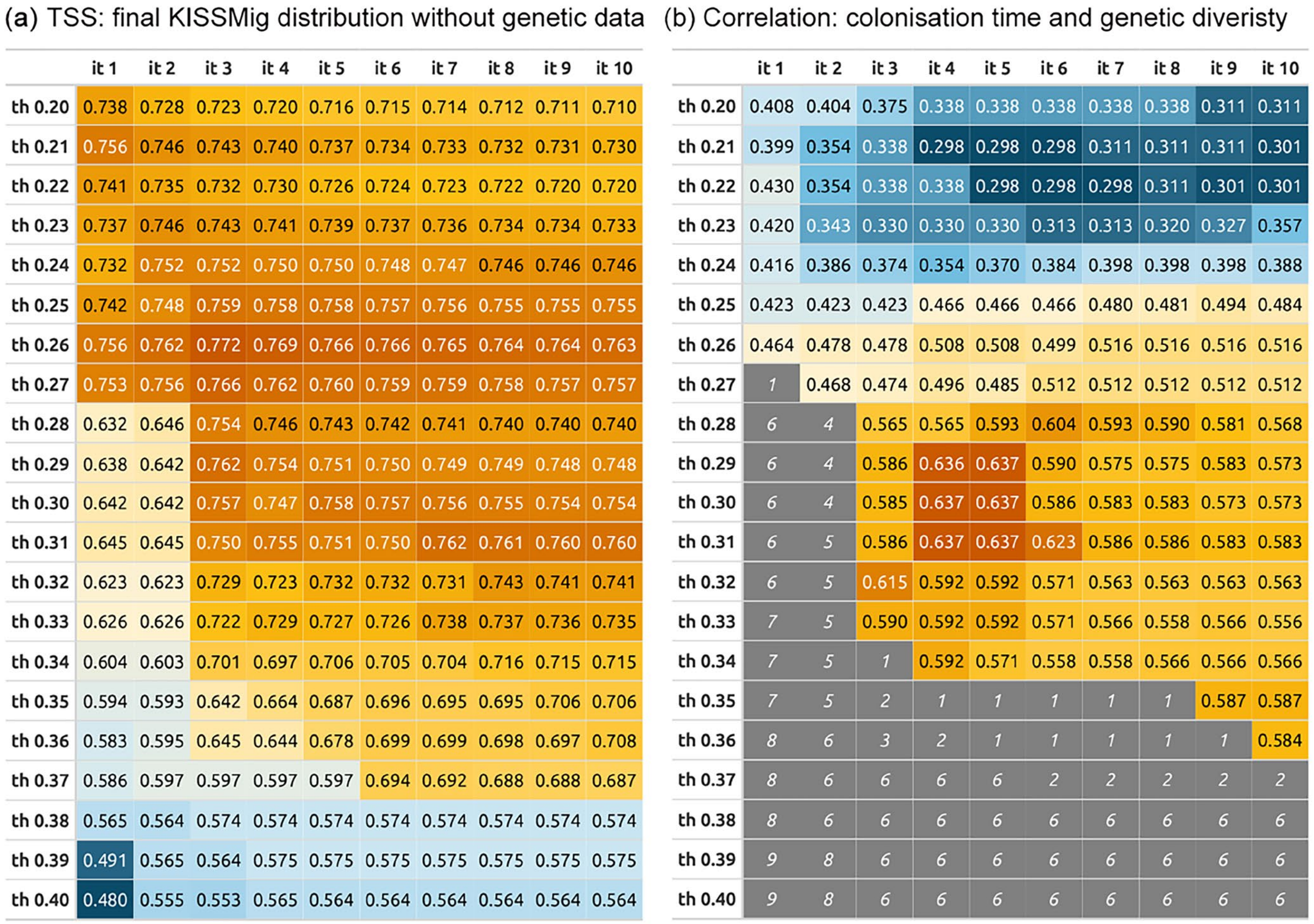

(a) TSS: final KISSMig distribution without genetic data

| | it 1 | it 2 | it 3 | it 4 | it 5 | it 6 | it 7 | it 8 | it 9 | it 10 |
|---|---|---|---|---|---|---|---|---|---|---|
| **th 0.20** | 0.738 | 0.728 | 0.723 | 0.720 | 0.716 | 0.715 | 0.714 | 0.712 | 0.711 | 0.710 |
| **th 0.21** | 0.756 | 0.746 | 0.743 | 0.740 | 0.737 | 0.734 | 0.733 | 0.732 | 0.731 | 0.730 |
| **th 0.22** | 0.741 | 0.735 | 0.732 | 0.730 | 0.726 | 0.724 | 0.723 | 0.722 | 0.720 | 0.720 |
| **th 0.23** | 0.737 | 0.746 | 0.743 | 0.741 | 0.739 | 0.737 | 0.736 | 0.734 | 0.734 | 0.733 |
| **th 0.24** | 0.732 | 0.752 | 0.752 | 0.750 | 0.750 | 0.748 | 0.747 | 0.746 | 0.746 | 0.746 |
| **th 0.25** | 0.742 | 0.748 | 0.759 | 0.758 | 0.758 | 0.757 | 0.756 | 0.755 | 0.755 | 0.755 |
| **th 0.26** | 0.756 | 0.762 | 0.772 | 0.769 | 0.766 | 0.766 | 0.765 | 0.764 | 0.764 | 0.763 |
| **th 0.27** | 0.753 | 0.756 | 0.766 | 0.762 | 0.760 | 0.759 | 0.759 | 0.758 | 0.757 | 0.757 |
| **th 0.28** | 0.632 | 0.646 | 0.754 | 0.746 | 0.743 | 0.742 | 0.741 | 0.740 | 0.740 | 0.740 |
| **th 0.29** | 0.638 | 0.642 | 0.762 | 0.754 | 0.751 | 0.750 | 0.749 | 0.749 | 0.748 | 0.748 |
| **th 0.30** | 0.642 | 0.642 | 0.757 | 0.747 | 0.758 | 0.757 | 0.756 | 0.755 | 0.754 | 0.754 |
| **th 0.31** | 0.645 | 0.645 | 0.750 | 0.755 | 0.751 | 0.750 | 0.762 | 0.761 | 0.760 | 0.760 |
| **th 0.32** | 0.623 | 0.623 | 0.729 | 0.723 | 0.732 | 0.732 | 0.731 | 0.743 | 0.741 | 0.741 |
| **th 0.33** | 0.626 | 0.626 | 0.722 | 0.729 | 0.727 | 0.726 | 0.738 | 0.737 | 0.736 | 0.735 |
| **th 0.34** | 0.604 | 0.603 | 0.701 | 0.697 | 0.706 | 0.705 | 0.704 | 0.716 | 0.715 | 0.715 |
| **th 0.35** | 0.594 | 0.593 | 0.642 | 0.664 | 0.687 | 0.696 | 0.695 | 0.695 | 0.706 | 0.706 |
| **th 0.36** | 0.583 | 0.595 | 0.645 | 0.644 | 0.678 | 0.699 | 0.699 | 0.698 | 0.697 | 0.708 |
| **th 0.37** | 0.586 | 0.597 | 0.597 | 0.597 | 0.597 | 0.694 | 0.692 | 0.688 | 0.688 | 0.687 |
| **th 0.38** | 0.565 | 0.564 | 0.574 | 0.574 | 0.574 | 0.574 | 0.574 | 0.574 | 0.574 | 0.574 |
| **th 0.39** | 0.491 | 0.565 | 0.564 | 0.575 | 0.575 | 0.575 | 0.575 | 0.575 | 0.575 | 0.575 |
| **th 0.40** | 0.480 | 0.555 | 0.553 | 0.565 | 0.564 | 0.564 | 0.564 | 0.564 | 0.564 | 0.564 |

(b) Correlation: colonisation time and genetic diveristy

| | it 1 | it 2 | it 3 | it 4 | it 5 | it 6 | it 7 | it 8 | it 9 | it 10 |
|---|---|---|---|---|---|---|---|---|---|---|
| **th 0.20** | 0.408 | 0.404 | 0.375 | 0.338 | 0.338 | 0.338 | 0.338 | 0.338 | 0.311 | 0.311 |
| **th 0.21** | 0.399 | 0.354 | 0.338 | 0.298 | 0.298 | 0.298 | 0.311 | 0.311 | 0.311 | 0.301 |
| **th 0.22** | 0.430 | 0.354 | 0.338 | 0.338 | 0.298 | 0.298 | 0.298 | 0.311 | 0.301 | 0.301 |
| **th 0.23** | 0.420 | 0.343 | 0.330 | 0.330 | 0.330 | 0.313 | 0.313 | 0.320 | 0.327 | 0.357 |
| **th 0.24** | 0.416 | 0.386 | 0.374 | 0.354 | 0.370 | 0.384 | 0.398 | 0.398 | 0.398 | 0.388 |
| **th 0.25** | 0.423 | 0.423 | 0.423 | 0.466 | 0.466 | 0.466 | 0.480 | 0.481 | 0.494 | 0.484 |
| **th 0.26** | 0.464 | 0.478 | 0.478 | 0.508 | 0.508 | 0.499 | 0.516 | 0.516 | 0.516 | 0.516 |
| **th 0.27** | *1* | 0.468 | 0.474 | 0.496 | 0.485 | 0.512 | 0.512 | 0.512 | 0.512 | 0.512 |
| **th 0.28** | *6* | *4* | 0.565 | 0.565 | 0.593 | 0.604 | 0.593 | 0.590 | 0.581 | 0.568 |
| **th 0.29** | *6* | *4* | 0.586 | 0.636 | 0.637 | 0.590 | 0.575 | 0.575 | 0.583 | 0.573 |
| **th 0.30** | *6* | *4* | 0.585 | 0.637 | 0.637 | 0.586 | 0.583 | 0.583 | 0.573 | 0.573 |
| **th 0.31** | *6* | *5* | 0.586 | 0.637 | 0.637 | 0.623 | 0.586 | 0.586 | 0.583 | 0.583 |
| **th 0.32** | *6* | *5* | 0.615 | 0.592 | 0.592 | 0.571 | 0.563 | 0.563 | 0.563 | 0.563 |
| **th 0.33** | *7* | *5* | 0.590 | 0.592 | 0.592 | 0.571 | 0.566 | 0.558 | 0.566 | 0.556 |
| **th 0.34** | *7* | *5* | *1* | 0.592 | 0.571 | 0.558 | 0.558 | 0.566 | 0.566 | 0.566 |
| **th 0.35** | *7* | *5* | *2* | *1* | *1* | *1* | *1* | *1* | 0.587 | 0.587 |
| **th 0.36** | *8* | *6* | *3* | *2* | *1* | *1* | *1* | *1* | *1* | 0.584 |
| **th 0.37** | *8* | *6* | *6* | *6* | *6* | *2* | *2* | *2* | *2* | *2* |
| **th 0.38** | *8* | *6* | *6* | *6* | *6* | *6* | *6* | *6* | *6* | *6* |
| **th 0.39** | *9* | *8* | *6* | *6* | *6* | *6* | *6* | *6* | *6* | *6* |
| **th 0.40** | *9* | *8* | *6* | *6* | *6* | *6* | *6* | *6* | *6* | *6* |

**FIGURE 6** | Optimisation matrices of KISSMig simulations with different combinations of iteration number per 100-year step (it, columns) and the suitability threshold (th, rows). The performance measures are: (a) true skill statistic of the simulated present-day distributions based on the current presence–pseudo-absence data, and (b) the average Spearman correlation between the four genetic diversity measures and the cumulative colonisation time at the locations of the 14 investigated populations. The four genetic diversity measures are nuclear genet diversity represented by simple sequence repeats (nSSRs), nuclear allelic richness, chloroplast gene diversity represented by simple sequence repeats (cpSSRs), and chloroplast haplotype richness. The numbers in italics on a grey background in matrix (b) show the number of populations that were not accessible for the given parameter values during the simulations. No correlations were calculated for these parameter settings. The colour gradient from blue to red corresponds to increasing TSS values and correlation strength respectively.

*Draco dussumieri* (Chaitanya et al. 2025); both studies attribute this pattern to rainfall regimes and adaptation to local climate. With the nSSRs clusters in our study, the Palakkad gap did not appear as a strong barrier in the past, and the admixture-like pattern of nuclear genetic clusters is an indicator of a historical connection between the two sides of the Palakkad gap. The within-group structure of *P. nigrum* from $K=4$ to $K=7$ indicates, however, limited gene flow below and above the Palakkad gap in recent times.

The chloroplast haplotypes H23 and H31 shared among Sirsi (P11), Coorg (P6) and Periyar (P2) populations and between Ponmudi (P1) and Coorg (P6) populations, respectively, support a possible genetic exchange through the lowlands (Appendix S4, Figure S4.8) which is also indicated by the genetically informed DSDM. Macro-remains of coastal moist forest elements recovered from the western slopes of the Western Ghats (Farooqui et al. 2010, 2014) likewise confirm a lowland connection between the two sides of the Palakkad gap. Such forests along the coast might have favoured species dispersal across the Western Ghats. In addition, the phylogenetically distinct haplotypes in the central Western Ghats suggest adaptation or re-expansion to new habitats, meaning that the populations of this area might have experienced the highest impact of climate change since the LGM, compared with the southern Western Ghats populations under a more widespread suitable climate. Although refugial areas in the north of the present species distribution lacked support from the cpSSRs and nSSRs, and the genetically informed DSDM, their existence is possible, but they might not have been effective refugia for the modern genetic structure.

Until c. 15,000 BP, our results support that *P. nigrum* has colonised in a rather dry climate the exposed land area during the period of low sea level. Still, the wetter conditions afterward might have opened new colonisation opportunities increasingly limited by the rising sea level. It is reasonable to assume that these dynamics were followed by a clear fragmentation of the species' range over the last c. 5000 years.

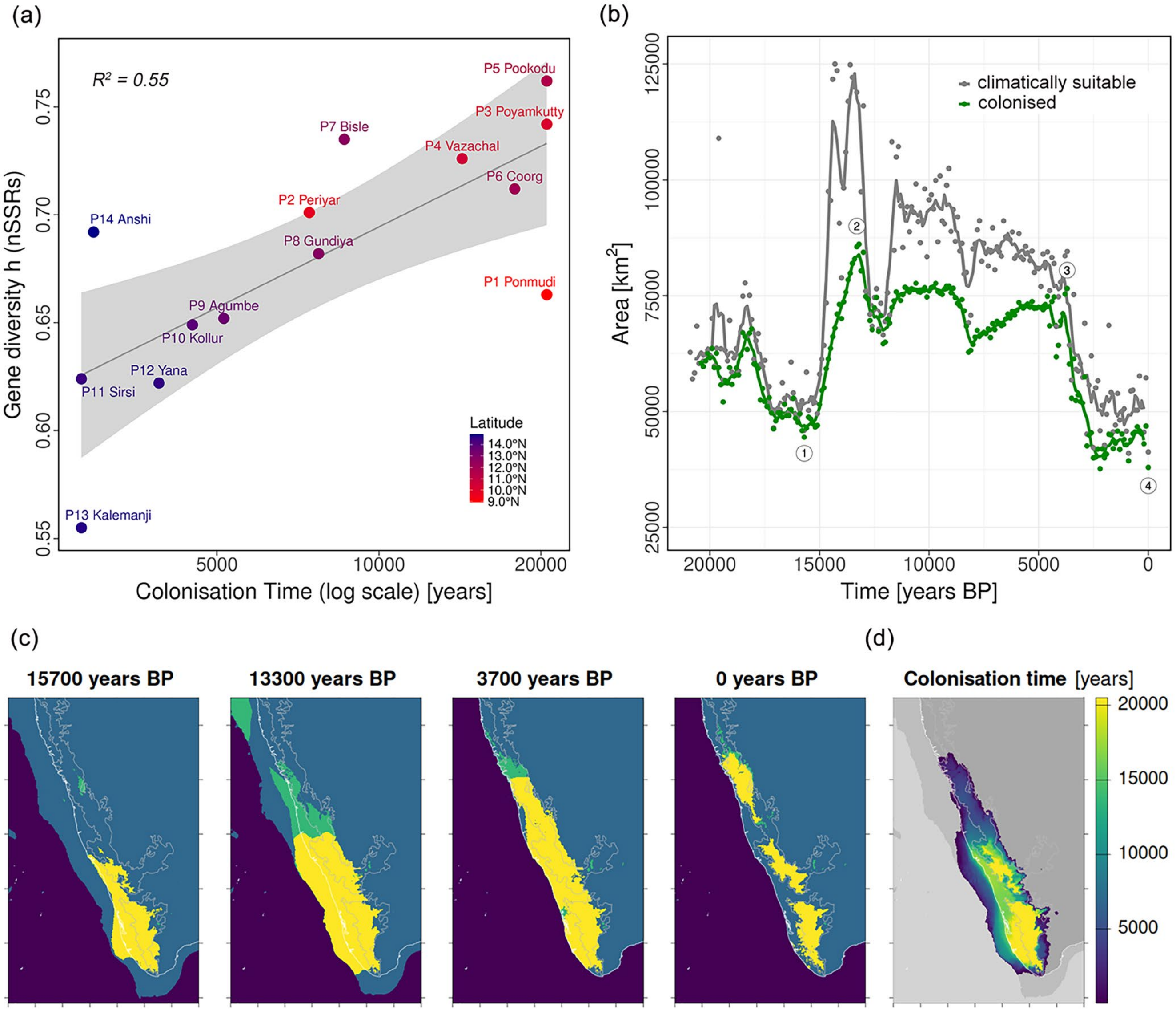

**FIGURE 7** | (a) Relationship between simulated cumulative colonisation time (log scale) of the genetically informed DSDM (suitability threshold = 0.29, iteration number = 4) and nuclear gene diversity (heterozygosity) among the 14 populations of *P. nigrum*. The solid line represents linear regression, and the shaded grey indicates its 95% confidence intervals. (b) Colonised area versus the climatically suitable area for the genetically informed DSDM. Area for each 100-year timestep, with lines calculated as the running average over 500 years. The numbers in the circles in (b) correspond to the four maps in (c), in which the colonised area is shown in yellow, climatically suitable but uncolonised area in green, and the blue colours distinguish between land and sea. (d) The final map shows the cumulative colonisation time of all timesteps. The grey lines represent the Western Ghats and the present coastline for comparison.

## 4.2 | Dynamic Species Distribution Modelling Informed by Population Genetics

In our DSDM framework, we evaluated different threshold values of climate suitability, which can be interpreted as testing different widths of the species' climatic niche—with higher threshold values describing a narrower niche. Along with the variation in the KISSMig iteration number, our simulations considered two fundamental species characteristics related to distribution dynamics: the width of the climate niche and the migration ability of the species. Solely based on the current presence–pseudo-absence data, the KISSMig simulations showed a high level of uncertainty for the optimised combination of the estimated niche width and migration ability. In contrast, the genetically informed approach revealed a pronounced and shifted correlation optimum and therefore provides stronger support for the selected simulation. These results differ from the rather narrow estimate of the migration ability without a genetically informed optimisation in Nobis and Normand (2014), which was facilitated by the missing range filling of the analysed tree species. With the predicted shrinking distribution of *P. nigrum* over the last millennia, however, it is hardly possible to estimate a more reliable migration rate based solely on the present species distribution. Improved estimates are nevertheless possible when genetic diversity is considered, as they also reflect past dynamics, including range expansions. This clearly demonstrates the ability of the genetically informed DSDM to reduce uncertainty in the estimated model parameters and to generate a more reliable reconstruction of the past distribution dynamics. It also opens an interesting research avenue for population geneticists and macroecologists to generate and test hypotheses on patterns of genetic diversity and species distributions across space and time.

Independent from the optimisation of the genetically informed DSDM, there exists additional support for the chosen simulation. Although we need to be aware of several sources of uncertainty in the ABC inferences including divergence time (Tsuda et al. 2015), the estimated divergence time between the two genetically distinct groups of the southern and central Western Ghats falls between 14,370 and 23,950 years BP, which matches the start of the northward expansion from a small distribution area around 15,000 BP in our simulation. In addition, the KISSMig iteration number of the genetically informed DSDM (it = 4) corresponds to an ecologically meaningful migration rate of 4,000 m per 100-year timestep. Assuming an average generation time of 4 years, this translates to an average dispersal distance of 160 m/generation (or 120 and 200 m if we assume five-year and three-year generation times, respectively). Although we are not aware of a study on *P. nigrum* dispersal distances, these values fit well with distances of seed dispersal by birds reported for other plant species (Weir and Corlett 2007; Rehm et al. 2019). Furthermore, the migration rate of *P. nigrum*, as an understory, clonally propagated species, is most likely affected not only by the generation time and dispersal, but also by the expansion rate of the tropical forest habitat. Finally, we notice that pollen is most likely not a major vector for nuclear DNA, as *P. nigrum* is mostly self-pollinated with instances of apomixis.

### 4.3 | Conservation Implications

In the context of current global change, unveiling genetic diversity hotspots and species distribution history, along with evaluations of a species' climate niche and migration ability, offers new insights for future conservation (see Keppel et al. 2015). From our genetic analysis, we identified two northern populations (Bisle (P7) and Anshi (P14)) of *Piper nigrum* from relatively undisturbed, protected habitats as reservoirs of genetic diversity. Although southern populations contributed less to overall nuclear diversity, they exhibited higher gene diversity and allelic richness at chloroplast loci, likely due to lower dispersal. Several morphological variants were observed within these populations (personal observation by TD and SS), underscoring their value for enhancing trait diversity in both *ex situ* collections and in situ conservation. Parts of the LGM refugial areas, indicated in our study by high genetic diversity and long colonisation time, fall near the existing network of protected areas (see Appendix S5). In these areas, we propose collecting seeds for seed bank and live specimens to preserve the genetic diversity of this important crop species. Despite regional variation in genetic patterns, we recommend establishing in situ conservation strategies to safeguard these genetic resources, because the species is known to be threatened due to habitat fragmentation from land-use changes, climate change, along with additional threats from pest infestations (Sen et al. 2016; Prathapan and Viraktamath 2008; Ravindran 2003).

### 4.4 | Limitations

The genetically informed DSDM developed in this study is novel and has not been tested with other species so far, although the approach can be integrated into genetic and macroecological studies of any taxon of interest. We are also not aware of the performance of this approach for species that show more complex distribution dynamics, such as large-scale hybridisation or secondary contact zones. The unclear correlation of cpSSR gene diversity with DSDM simulations may result from such secondary contact and lineage mixing during post-LGM colonisation, as shown by Petit et al. (2003). Such cases would require further investigations and could provide opportunities for improvements to the approach. Finally, our DSDMs predicted, outside of the study area, climatically suitable habitats also for Sri Lanka. These habitats were not connected to suitable areas in our simulations, but this could be investigated further in the future (see Metschina et al. 2025).

## 5 | Conclusions

Overall, our study demonstrates how the integration of paleoclimate modelling, dynamic species distribution modelling, and population genetics can provide better insights for understanding population genetic and phylogeographic patterns, identify areas of high genetic diversity, and provide novel biogeographic explanations for the climate-related dynamics of biodiversity. We identified multiple effective refugial areas within the Western Ghats', where the coastal lowlands once acted as an important migration route for evergreen species such as *P. nigrum*. Although we employed gene diversity, haplotype richness, and allelic richness as genetic diversity indices in our genetically informed DSDM, the approach developed here should also be applicable to other genetic diversity measures, such as nucleotide diversity, $F_{ST}$, or effective population size obtained from population genomic data.

---

**Author Contributions**

**Sandeep Sen:** conceptualisation (equal), formal analysis (genetics) (lead), investigation (lead), methodology (lead), validation (lead), funding acquisition (lead), visualisation (lead), writing – original draft (lead), writing – review and editing (lead). **Michael Peter Nobis:** conceptualisation (equal); formal analysis (DSDMs) (lead), investigation (lead), methodology (lead), validation (lead), visualisation (lead), writing – original draft (lead), writing – review and editing (lead). **Rani M. S. Saggere:** data curation (supporting), writing – review and editing (supporting). **Srirama Ramanujam:** data curation (supporting), funding acquisition (supporting), writing – review and editing (supporting). **Thomson Davis:** data curation (supporting), writing – review and editing (supporting). **Dirk Nikolaus Karger:** methodology (supporting), resources (supporting), writing – review and editing (supporting). **G. Ravikanth:** conceptualisation (equal), supervision (lead), methodology (lead), validation (lead), funding acquisition (lead), writing – review and editing (supporting). **Yoshiaki Tsuda:** conceptualisation (equal), formal analysis (equal), investigation (lead), supervision (lead), funding acquisition (lead), methodology (lead), validation (lead), visualisation (lead), writing – original draft (supporting), writing – review and editing (equal).

## Acknowledgements

S.S., T.D. and G.R. thank the Forest departments of Kerala (WL10-32824) and Karnataka (PCCF/C/GL-276/2014-15 and PCCF (WL)/E2/CR-34/2015-16) for permission to conduct field work. S.S., Y.T., and G.R. thank the National Biodiversity Authority (NBA/Tech Appl/9/FormB-176/20/20-21/2959NBA) India for supporting this study. We acknowledge the late Christopher Davidson, Jagadish M. R. and Ganesan R. for their support. We thank Mellisa Dawes for proofreading the initial manuscript of this work.

## Conflicts of Interest

The authors declare no conflicts of interest.

## Data Availability Statement

The R scripts of the dynamic modelling and the datasets used in this study are available in the Supporting Information. The paleoclimate data of CHELSA-TraCE21k are available on the CHELSA portal (https://chelsa-climate.org/). The genetic data generated during this study are available in the Dryad Digital Repository https://doi.org/10.5061/dryad.d2547d8fm

## Peer Review

The peer review history for this article is available at https://www.webofscience.com/api/gateway/wos/peer-review/10.1111/ddi.70070.

## References

Bellard, C., C. Bertelsmeier, P. Leadley, W. Thuiller, and F. Courchamp. 2012. "Impacts of Climate Change on the Future of Biodiversity." *Ecology Letters* 15, no. 4: 365–377. https://doi.org/10.1111/j.1461-0248.2011.01736.x.

Bocedi, G., S. C. F. Palmer, A.-K. Malchow, D. Zurell, K. Watts, and J. M. J. Travis. 2021. "RangeShifter 2.0: An Extended and Enhanced Platform for Modelling Spatial Eco-Evolutionary Dynamics and Species' Responses to Environmental Changes." *Ecography* 44: 1453–1462.

Bocedi, G., S. C. F. Palmer, G. Pe'er, et al. 2014. "RangeShifter: A Platform for Modelling Spatial Eco-Evolutionary Dynamics and Species' Responses to Environmental Changes." *Methods in Ecology and Evolution* 5: 388–396.

Bodare, S., Y. Tsuda, G. Ravikanth, R. Uma Shaanker, and M. Lascoux. 2013. "Genetic Structure and Demographic History of the Endangered Tree Species *Dysoxylum malabaricum* (Meliaceae) in Western Ghats, India: Implications for Conservation in a Biodiversity Hotspot." *Ecology and Evolution* 3: 3233–3248. https://doi.org/10.1002/ece3.669.

Boria, R. A., and J. L. Blois. 2023. "Phylogeography Within the *Peromyscus maniculatus* Species Group: Understanding Past Distribution of Genetic Diversity and Areas of Refugia in Western North America." *Molecular Phylogenetics and Evolution* 180: 107701. https://doi.org/10.1016/j.ympev.2023.107701.

Bose, R., F. Munoz, B. R. Ramesh, and R. Pélissier. 2016. "Past Potential Habitats Shed Light on the Biogeography of Endemic Tree Species of the Western Ghats Biodiversity Hotspot, South India." *Journal of Biogeography* 43: 899–910. https://doi.org/10.1111/jbi.12682.

Breiner, F. T., A. Guisan, A. Bergamini, and M. P. Nobis. 2015. "Overcoming Limitations of Modelling Rare Species by Using Ensembles of Small Models." *Methods in Ecology and Evolution* 6: 1210–1218. https://doi.org/10.1111/2041-210X.12403.

Brown, J. L., J. J. Weber, D. F. Alvarado-Serrano, M. J. Hickerson, S. J. Franks, and A. C. Carnaval. 2016. "Predicting the Genetic Consequences of Future Climate Change: The Power of Coupling Spatial Demography, the Coalescent, and Historical Landscape Changes." *American Journal of Botany* 103: 153–163. https://doi.org/10.3732/ajb.1500117.

Bryant, D., and V. Moulton. 2004. "Neighbor-Net: An Agglomerative Method for the Construction of Phylogenetic Networks." *Molecular Biology and Evolution* 21: 255–265. https://doi.org/10.1093/molbev/msh018.

Castilla, A. R., A. Brown, S. Hoban, et al. 2024. "Integrative Demographic Modelling Reduces Uncertainty in Estimated Rates of Species' Historical Range Shifts." *Journal of Biogeography* 51: 325–336. https://doi.org/10.1111/jbi.14754.

Chaitanya, R., A. Dhibar, A. Khandekar, C. Murthy, S. Meiri, and P. Karanth. 2025. "Speciation in the Peninsular Indian Flying Lizard (*Draco dussumieri*) Follows Climatic Transition and Not Physical Barriers." *Molecular Ecology* 34: e17800.

Chiocchio, A., J. W. Arntzen, I. Martínez-Solano, et al. 2021. "Reconstructing Hotspots of Genetic Diversity From Glacial Refugia and Subsequent Dispersal in Italian Common Toads (*Bufo bufo*)." *Scientific Reports* 11: 260. https://doi.org/10.1038/s41598-020-79046-y.

Cincotta, R. P., J. Wisnewski, and R. Engelman. 2000. "Human Population in the Biodiversity Hotspots." *Nature* 404: 990–992. https://doi.org/10.1038/35010105.

Comps, B., D. Gömöry, J. Letouzey, B. Thiébaut, and R. J. Petit. 2001. "Diverging Trends Between Heterozygosity and Allelic Richness During Postglacial Colonization in the European Beech." *Genetics* 157: 389–397. https://doi.org/10.1093/genetics/157.1.389.

Corlett, R. T., and D. A. Westcott. 2013. "Will Plant Movements Keep Up With Climate Change?" *Trends in Ecology & Evolution* 28: 482–488. https://doi.org/10.1016/j.tree.2013.04.003.

Cornuet, J.-M., P. Pudlo, J. Veyssier, et al. 2014. "DIYABC v2.0: A Software to Make Approximate Bayesian Computation Inferences About Population History Using Single Nucleotide Polymorphism, DNA Sequence and Microsatellite Data." *Bioinformatics* 30: 1187–1189. https://doi.org/10.1093/bioinformatics/btt763.

Cornuet, J.-M., F. Santos, M. A. Beaumont, et al. 2008. "Inferring Population History With DIYABC: A User-Friendly Approach to Approximate Bayesian Computation." *Bioinformatics* 24: 2713–2719. https://doi.org/10.1093/bioinformatics/btn514.

Das, A., J. Krishnaswamy, K. S. Bawa, et al. 2006. "Prioritisation of Conservation Areas in the Western Ghats, India." *Biological Conservation* 133: 16–31. https://doi.org/10.1016/j.biocon.2006.05.023.

Davis, T. 2017. "Biosystematic Studies on *Piper* Species of Kerala—Forests With Special Reference to Intraspecific Variants of the Wild *Piper nigrum* L." Ph.D. Thesis. Kannur University, Kerala, India.

Dobson, R., A. J. Challinor, R. A. Cheke, S. Jennings, S. G. Willis, and M. Dallimer. 2023. "dynamicSDM: An R Package for Species Geographical Distribution and Abundance Modelling at High Spatiotemporal Resolution." *Methods in Ecology and Evolution* 14: 1190–1199.

Dormann, C. F., J. Elith, S. Bacher, et al. 2013. "Collinearity: A Review of Methods to Deal With It and a Simulation Study Evaluating Their Performance." *Ecography* 36: 27–46. https://doi.org/10.1111/j.1600-0587.2012.07348.x.

Dupanloup, I., S. Schneider, and L. Excoffier. 2002. "A Simulated Annealing Approach to Define the Genetic Structure of Populations." *Molecular Ecology* 11: 2571–2581. https://doi.org/10.1046/j.1365-294X.2002.01650.x.

El-Mousadik, A., and R. J. Petit. 1996. "High Level of Genetic Differentiation for Allelic Richness Among Populations of the Argan Tree [Argania Spinosa (L.) Skeels] Endemic to Morocco." *Theoretical and Applied Genetics* 92: 832–839. https://doi.org/10.1007/BF00221895.

Engler, R., and A. Guisan. 2009. "MigClim: Predicting Plant Distribution and Dispersal in a Changing Climate." *Diversity and Distributions* 15: 590–601.

Espíndola, A., L. Pellissier, L. Maiorano, W. Hordijk, A. Guisan, and N. Alvarez. 2012. "Predicting Present and Future Intra-Specific Genetic Structure Through Niche Hindcasting Across 24 Millennia." *Ecology Letters* 15: 649–657. https://doi.org/10.1111/j.1461-0248.2012.01779.x.

Evanno, G., S. Regnaut, and J. Goudet. 2005. "Detecting the Number of Clusters of Individuals Using the Software STRUCTURE: A Simulation Study." *Molecular Ecology* 14: 2611–2620. https://doi.org/10.1111/j.1365-294X.2005.02553.x.

Falush, D., M. Stephens, and J. K. Pritchard. 2007. "Inference of Population Structure Using Multilocus Genotype Data: Dominant Markers and Null Alleles." *Molecular Ecology Notes* 7: 574–578. https://doi.org/10.1111/j.1471-8286.2007.01758.x.

Farooqui, A., J. N. Pattan, G. Parthiban, J. Srivastava, and R. Ranjana. 2014. "Palynological Record of Tropical Rain Forest Vegetation and Sea Level Fluctuations Since 140 Ka From Sediment Core, South-Eastern Arabian Sea." *Palaeogeography, Palaeoclimatology, Palaeoecology* 411: 95–109. https://doi.org/10.1016/j.palaeo.2014.06.020.

Farooqui, A., J. G. Ray, S. A. Farooqui, R. K. Tiwari, and Z. A. Khan. 2010. "Tropical Rainforest Vegetation, Climate, and Sea Level During the Pleistocene in Kerala, India." *Quaternary International* 213: 2–11. https://doi.org/10.1016/j.quaint.2009.09.024.

Flantua, S. G. A., A. O'Dea, R. E. Onstein, C. Giraldo, and H. Hooghiemstra. 2019. "The Flickering Connectivity System of the North Andean Páramos." *Journal of Biogeography* 46: 1808–1825. https://doi.org/10.1111/jbi.13607.

Franklin, J. 2023. "Species Distribution Modelling Supports the Study of Past, Present, and Future Biogeographies." *Journal of Biogeography* 50: 1533–1545. https://doi.org/10.1111/jbi.14617.

Goldstein, D. B., A. Ruiz Linares, L. L. Cavalli-Sforza, and M. W. Feldman. 1995. "Genetic Absolute Dating Based on Microsatellites and the Origin of Modern Humans." *Proceedings of the National Academy of Sciences* 92: 6723–6727. https://doi.org/10.1073/pnas.92.15.6723.

Gopal, A., D. K. Bharti, N. Page, et al. 2023. "Range-Restricted Old and Young Lineages Show the Southern Western Ghats to Be Both a Museum and a Cradle of Diversity for Woody Plants." *Proceedings of the Royal Society B: Biological Sciences* 290: 20222513. https://doi.org/10.1098/rspb.2022.2513.

Gotelli, N. J., and J. Stanton-Geddes. 2015. "Climate Change, Genetic Markers, and Species Distribution Modelling." *Proceedings of the Royal Society B: Biological Sciences* 42: 1577–1585. https://doi.org/10.1098/rspb.2019.04862015.

Guisan, A., W. Thuiller, and N. E. Zimmermann. 2017. *Habitat Suitability and Distribution Models: With Applications in R*. Cambridge University Press. https://doi.org/10.1017/9781139028271.

Hedrick, P. W. 2005. "A Standardized Genetic Differentiation Measure." *Evolution* 59: 1633–1638. https://doi.org/10.1111/j.0014-3820.2005.tb01814.x.

Hernández, N. A. H., Á. L. R. Fernández, and N. Upham. 2024. "Environmental Suitability Throughout the Late Quaternary Explains Population Genetic Diversity." *Ecography* 2025: e07202.

Hijmans, R. J. 2019. "Geosphere: Spherical trigonometry (Version 1.5–10) [R package]." https://CRAN.R-project.org/package=geosphere.

Hoban, S. M., D. S. Borkowski, S. L. Brosi, et al. 2010. "Range-Wide Distribution of Genetic Diversity in the North American Tree *Juglans cinerea*: A Product of Range Shifts, Not Ecological Marginality or Recent Population Decline." *Molecular Ecology* 19: 4876–4891. https://doi.org/10.1111/j.1365-294X.2010.04834.x.

Hubisz, M. J., D. Falush, M. Stephens, and J. K. Pritchard. 2009. "Inferring Weak Population Structure With the Assistance of Sample Group Information." *Molecular Ecology Resources* 9: 1322–1332. https://doi.org/10.1111/j.1755-0998.2009.02591.x.

Huson, D. H., and D. Bryant. 2006. "Application of Phylogenetic Networks in Evolutionary Studies." *Molecular Biology and Evolution* 23: 254–267. https://doi.org/10.1093/molbev/msj030.

Karger, D. N., M. P. Nobis, S. Normand, C. H. Graham, and N. E. Zimmermann. 2021. *CHELSA-TraCE21k: Downscaled Transient Temperature and Precipitation Data Since the Last Glacial Maximum*. Envidat. https://doi.org/10.16904/envidat.211.

Karger, D. N., M. P. Nobis, S. Normand, C. H. Graham, and N. E. Zimmermann. 2023. "CHELSA-TraCE21k–High-Resolution (1 Km) Downscaled Transient Temperature and Precipitation Data Since the Last Glacial Maximum." *Climate of the Past* 19: 439–456. https://doi.org/10.5194/cp-19-439-2023.

Keppel, G., K. Mokany, G. W. Wardell-Johnson, B. L. Phillips, J. A. Welbergen, and A. E. Reside. 2015. "The Capacity of Refugia for Conservation Planning Under Climate Change." *Frontiers in Ecology and the Environment* 13: 106–112. https://doi.org/10.1890/140055.

Kirschner, P., M. Perez, E. Záveská, et al. 2022. "Congruent Evolutionary Responses of European Steppe Biota to Late Quaternary Climate Change." *Nature Communications* 13: 1921. https://doi.org/10.1038/s41467-022-29267-8.

Kirschner, P., E. Záveská, K. Hülber, et al. 2023. "Evolutionary Dynamics of *Euphorbia Carniolica* Suggest a Complex Plio–Pleistocene History of Understorey Species of Deciduous Forest in Southeastern Europe." *Molecular Ecology* 32: 5350–5368. https://doi.org/10.1111/mec.17102.

Langella, O. 1999. "Populations 1.2.3." Bioinformatics. https://bioinformatics.org/populations/.

Lee-Yaw, J. A., L. J. McCune, S. Pironon, and N. S. Sheth. 2022. "Species Distribution Models Rarely Predict the Biology of Real Populations." *Ecography* 2022: e05877. https://doi.org/10.1111/ecog.05877.

Leugger, F., T. Broquet, D. N. Karger, et al. 2022. "Dispersal and Habitat Dynamics Shape the Genetic Structure of the Northern Chamois in the Alps." *Journal of Biogeography* 49: 1848–1861. https://doi.org/10.1111/jbi.14363.

López-Cortegano, E., A. Pérez-Figueroa, and A. Caballero. 2019. "Metapop 2: Re-Implementation of Software for the Analysis and Management of Subdivided Populations Using Gene and Allelic Diversity." *Molecular Ecology Resources* 19: 1095–1100. https://doi.org/10.1111/1755-0998.13015.

Luna, L. W., L. N. Naka, G. Thom, et al. 2023. "Late Pleistocene Landscape Changes and Habitat Specialization as Promoters of Population Genomic Divergence in Amazonian Floodplain Birds." *Molecular Ecology* 32: 214–228. https://doi.org/10.1111/mec.16741.

Magri, D., G. G. Vendramin, B. Comps, et al. 2006. "A New Scenario for the Quaternary History of European Beech Populations: Palaeobotanical Evidence and Genetic Consequences." *New Phytologist* 171: 199–221. https://doi.org/10.1111/j.1469-8137.2006.01740.x.

Maiorano, L., R. Cheddadi, N. E. Zimmermann, et al. 2013. "Building the Niche Through Time: Using 13,000 Years of Data to Predict the Effects of Climate Change on Three Tree Species in Europe." *Global Ecology and Biogeography* 22: 302–317. https://doi.org/10.1111/j.1466-8238.2012.00767.x.

McGaughran, A. 2015. "Integrating a Population Genomics Focus Into Biogeographic and Macroecological Research." *Frontiers in Ecology and Evolution* 3: 132. https://doi.org/10.3389/fevo.2015.00132.

Meek, M. H., E. A. Beever, S. Barbosa, et al. 2023. "Understanding Local Adaptation to Prepare Populations for Climate Change." *Bioscience* 73: 36–47. https://doi.org/10.1093/biosci/biac101.

Meirmans, P. G. 2015. "Seven Common Mistakes in Population Genetics and How to Avoid Them." *Molecular Ecology* 24: 3223–3231. https://doi.org/10.1111/mec.13243.

Meirmans, P. G. 2020. “Genodive Version 3.0: Easy-To-Use Software for the Analysis of Genetic Data of Diploids and Polyploids.” *Molecular Ecology Resources* 20: 1126–1131. https://doi.org/10.1111/1755-0998.13145.

Meirmans, P. G., and P. W. Hedrick. 2011. “Assessing Population Structure: FST and Related Measures.” *Molecular Ecology Resources* 11: 5–718. https://doi.org/10.1111/j.1755-0998.2010.02927.x.

Menezes, I. D., F. W. Cidade, A. P. Souza, and I. C. Sampaio. 2009. “Isolation and Characterization of Microsatellite Loci in the Black Pepper, *Piper nigrum* L. (Piperaceae).” *Conservation Genetics Resources* 1: 209–212. https://doi.org/10.1007/s12686-009-9051-6.

Metschina, D., L. A. Cauz-Santos, M. J. Christenhusz, et al. 2025. “Origin and Biogeographical History of Palaeotropical Piper (Piperaceae): Multiple Long-Distance Dispersals From South America Initiated During the Middle Eocene Climatic Optimum.” *Botanical Journal of the Linnean Society*: boaf014. https://doi.org/10.1093/botlinnean/boaf014.

Morley, R. J. 2000. *Origin and Evolution of Tropical Rain Forests*. Wiley.

Myers, N., R. A. Mittermeier, C. G. Mittermeier, G. A. B. da Fonseca, and J. Kent. 2000. “Biodiversity Hotspots for Conservation Priorities.” *Nature* 403: 853–858. https://doi.org/10.1038/35002501.

Nair, R. R., S. Karumathil, P. S. Udayan, R. P. Prakashkumar, and A. N. Sérsic. 2019. “Evolutionary History of *Kingiodendron pinnatum* (Fabaceae: Caesalpinoideae), an Endangered Species of the Western Ghats, India: A Phylogeographical Approach.” *Biological Journal of the Linnean Society* 126: 688–705. https://doi.org/10.1093/biolinnean/blz004.

Nobis, M. P. 2024. “Kissmig: A Keep It Simple Species Migration Model. R Package Version 1.0–5.” https://CRAN.R-project.org/package=kissmig.

Nobis, M. P., and S. Normand. 2014. “KISSMig—A Simple Model for R to Account for Limited Migration in Analyses of Species Distributions.” *Ecography* 37: 1282–1287. https://doi.org/10.1111/ecog.00930.

Parks, D. H., T. Mankowski, S. Zangooei, et al. 2013. “GenGIS 2: Geospatial Analysis of Traditional and Genetic Biodiversity, With New Gradient Algorithms and an Extensible Plugin Framework.” *PLoS One* 8: e69885. https://doi.org/10.1371/journal.pone.0069885.

Peakall, R., and P. E. Smouse. 2006. “GENALEX 6: Genetic Analysis in Excel. Population Genetic Software for Teaching and Research.” *Molecular Ecology Notes* 6: 288–295. https://doi.org/10.1111/j.1471-8286.2005.01155.x.

Petit, R. J., I. Aguinagalde, J. L. de Beaulieu, et al. 2003. “Glacial Refugia: Hotspots but Not Melting Pots of Genetic Diversity.” *Science* 300: 1563–1565. https://doi.org/10.1126/science.1083264.

Petit, R. J., E. Pineau, B. Demesure, R. Bacilieri, A. Ducousso, and A. Kremer. 1997. “Chloroplast DNA Footprints of Postglacial Recolonization by Oaks.” *Proceedings of the National Academy of Sciences* 94: 9996–10001. https://doi.org/10.1073/pnas.94.18.9996.

Pons, O., and R. J. Petit. 1996. “Measuring and Testing Genetic Differentiation With Ordered Versus Unordered Alleles.” *Genetics* 144: 1237–1245. https://doi.org/10.1093/genetics/144.3.1237.

Prabhu, C. N., R. Shankar, K. Anupama, et al. 2004. “A 200-Ka Pollen and Oxygen-Isotopic Record From Two Sediment Cores From the Eastern Arabian Sea.” *Palaeogeography, Palaeoclimatology, Palaeoecology* 214: 309–321. https://doi.org/10.1016/j.palaeo.2004.07.027.

Prasad, V., A. Farooqui, S. K. M. Tripathi, R. Garg, and B. Thakur. 2009. “Evidence of Late Palaeocene–Early Eocene Equatorial Rainforest Refugia in Southern Western Ghats, India.” *Journal of Biosciences* 34: 777–797. https://doi.org/10.1007/s12038-009-0062-y.

Prathapan, K. D., and C. A. Viraktamath. 2008. “The Flea Beetle Genus Lanka (Coleoptera: Chrysomelidae) in India With Descriptions of Three New Species and Notes on the Identity of the Pollu Beetle Infesting Black Pepper, *Piper nigrum*.” *Zootaxa* 1681: 1–30. https://doi.org/10.11646/zootaxa.1681.1.1.

Pritchard, J. K., M. Stephens, and P. Donnelly. 2000. “Inference of Population Structure Using Multilocus Genotype Data.” *Genetics* 155: 945–959. https://doi.org/10.1093/genetics/155.2.945.

Quinzin, M. C., S. Normand, S. Dellicour, J. C. Svenning, and P. Mardulyn. 2017. “Glacial Survival of Trophically Linked Boreal Species in Northern Europe.” *Proceedings of the Royal Society B: Biological Sciences* 284: 20162799. https://doi.org/10.1098/rspb.2016.2799.

R Core Team. 2024. *R: A Language and Environment for Statistical Computing*. R Foundation for Statistical Computing. https://www.R-project.org/.

Rao, P., and R. Kumar. 2022. “Evolution of the Western Ghats: Constraints From Receiver Function Imaging and Harmonic Decomposition.” *Tectonophysics* 838: 229472.

Ravindran, P. N., ed. 2003. *Black pepper: Piper nigrum*. CRC Press.

Rehm, E., E. Fricke, J. Bender, J. Savidge, and H. Rogers. 2019. “Animal Movement Drives Variation in Seed Dispersal Distance in a Plant–Animal Network.” *Proceedings of the Royal Society B: Biological Sciences* 286: 20182007. https://doi.org/10.1098/rspb.2018.2007.

Robin, V. V., A. Sinha, and U. Ramakrishnan. 2010. “Ancient Geographical Gaps and Paleo-Climate Shape the Phylogeography of an Endemic Bird in the Sky Islands of Southern India.” *PLoS One* 5: e13321. https://doi.org/10.1371/journal.pone.0013321.

Rousset, F. 1997. “Genetic Differentiation and Estimation of Gene Flow From F-Statistics Under Isolation by Distance.” *Genetics* 145: 1219–1228. https://doi.org/10.1093/genetics/145.4.1219.

Rubenstein, M. A., S. R. Weiskopf, R. Bertrand, et al. 2023. “Climate Change and the Global Redistribution of Biodiversity: Substantial Variation in Empirical Support for Expected Range Shifts.” *Environmental Evidence* 12, no. 1: 7. https://doi.org/10.1186/s13750-023-00296-0.

Sandel, B., C. Merow, J. M. Serra-Diaz, and J. Svenning. 2025. “Disequilibrium in Plant Distributions: Challenges and Approaches for Species Distribution Models.” *Journal of Ecology* 113: 782–794.

Sen, S., S. Dayanandan, T. Davis, et al. 2019. “Origin and Evolution of the Genus Piper in Peninsular India.” *Molecular Phylogenetics and Evolution* 138: 102–113. https://doi.org/10.1016/j.ympev.2019.05.033.

Sen, S., A. Gode, S. Ramanujam, G. Ravikanth, and N. A. Aravind. 2016. “Modeling the Impact of Climate Change on Wild *Piper nigrum* (Black Pepper) in Western Ghats, India Using Ecological Niche Models.” *Journal of Plant Research* 129: 1033–1040. https://doi.org/10.1007/s10265-016-0859-3.

Sen, S., and G. Rengaian. 2022. “A Review on the Ecology, Evolution and Conservation of Piper (Piperaceae) in India: Future Directions and Opportunities.” *Botanical Review* 88: 333–358. https://doi.org/10.1007/s12229-021-09269-9.

Shipley, B. R., R. Bach, Y. Do, H. Strathearn, J. L. McGuire, and B. Dilkina. 2022. “megaSDM: Integrating Dispersal and Time-Step Analyses Into Species Distribution Models.” *Ecography* 2022: e05450.

Smith, M. L., J. Wallace, D. C. Tank, J. Sullivan, and B. C. Carstens. 2022. “The Role of Multiple Pleistocene Refugia in Promoting Diversification in the Pacific Northwest.” *Molecular Ecology* 31: 4402–4416. https://doi.org/10.1111/mec.16595.

Strassburg, B. B. N., A. Iribarrem, H. L. Beyer, et al. 2020. “Global Priority Areas for Ecosystem Restoration.” *Nature* 586: 724–729. https://doi.org/10.1038/s41586-020-2784-9.

Svenning, J. C., and F. Skov. 2004. “Limited Filling of the Potential Range in European Tree Species.” *Ecology Letters* 7: 565–573. https://doi.org/10.1111/j.1461-0248.2004.00614.x.

Tiwari, M., A. K. Singh, and R. Ramesh. 2011. "High-Resolution Monsoon Records Since Last Glacial Maximum: A Comparison of Marine and Terrestrial Paleoarchives From South Asia." *Journal of Geological Research* 119: 1–12. https://doi.org/10.1155/2011/765248.

Tsuda, Y., J. Chen, M. Stocks, et al. 2016. "The Extent and Meaning of Hybridization and Introgression Between Siberian Spruce (*Picea obovata*) and Norway Spruce (*Picea abies*): Cryptic Refugia as Stepping Stones to the West?" *Molecular Ecology* 25: 2773–2789. https://doi.org/10.1111/mec.13654.

Tsuda, Y., K. Nakao, Y. Ide, and Y. Tsumura. 2015. "The Population Demography of *Betula maximowicziana*, a Cool-Temperate Tree Species in Japan, in Relation to the Last Glacial Period: Its Admixture-Like Genetic Structure Is the Result of Simple Population Splitting Not Admixing." *Molecular Ecology* 24: 1403–1418. https://doi.org/10.1111/mec.13123.

Tsuda, Y., V. Semerikov, F. Sebastiani, G. G. Vendramin, and M. Lascoux. 2017. "Multispecies Genetic Structure and Hybridization in the Betula Genus Across Eurasia." *Molecular Ecology* 26: 589–605. https://doi.org/10.1111/mec.13885.

Uribe-Rivera, D. E., G. Guillera-Arroita, S. M. Windecker, P. Pliscoff, and B. A. Wintle. 2023. "The Predictive Performance of Process-Explicit Range Change Models Remains Largely Untested." *Ecography* 2023, no. 4: e06048. https://doi.org/10.1111/ecog.06048.

Vijayakumar, S. P., R. C. Menezes, A. Jayarajan, and K. Shanker. 2016. "Glaciations, Gradients, and Geography: Multiple Drivers of Diversification of Bush Frogs in the Western Ghats Escarpment." *Proceedings of the Royal Society B: Biological Sciences* 283: 20161011. https://doi.org/10.1098/rspb.2016.1011.

Wang, Y., S. Pineda-Munoz, and J. L. McGuire. 2023. "Plants Maintain Climate Fidelity in the Face of Dynamic Climate Change." *Proceedings of the National Academy of Sciences of the United States of America* 120: e2201946119. https://doi.org/10.1073/pnas.2201946119.

Weir, J. E., and R. T. Corlett. 2007. "How Far Do Birds Disperse Seeds in the Degraded Tropical Landscape of Hong Kong, China?" *Landscape Ecology* 22: 131–140. https://doi.org/10.1007/s10980-006-9002-5.

Weising, K., and R. C. Gardner. 1999. "A Set of Conserved PCR Primers for the Analysis of Simple Sequence Repeat Polymorphisms in Chloroplast Genomes of Dicotyledonous Angiosperms." *Genome* 42: 9–19. https://doi.org/10.1139/g98-104.

Wright, S. 1943. "Isolation by Distance." *Genetics* 28: 114–138. https://doi.org/10.1093/genetics/28.2.114.

Yannic, G., O. Hagen, F. Leugger, D. N. Karger, and L. Pellissier. 2020. "Harnessing Paleo-Environmental Modeling and Genetic Data to Predict Intraspecific Genetic Structure." *Evolutionary Applications* 13: 1526–1542. https://doi.org/10.1111/eva.12986.

Yannic, G., L. Pellissier, J. Ortego, et al. 2014. "Genetic Diversity in Caribou Linked to Past and Future Climate Change." *Nature Climate Change* 4: 132–137. https://doi.org/10.1038/nclimate2074.

## Supporting Information

Additional supporting information can be found online in the Supporting Information section. **Appendix S1:** ddi70070-sup-0001-AppendixS1.docx. **Appendix S2:** ddi70070-sup-0002-AppendixS2.docx. **Appendix S3:** ddi70070-sup-0003-AppendixS3.docx. **Appendix S4:** ddi70070-sup-0004-AppendixS4.docx. **Appendix S5:** ddi70070-sup-0005-AppendixS5.docx.